MEASUREMENTS OF SKIN FRICTION IN TURBULENT BOUNDARY LAYERS AT TRANSONIC SPEEDS

Thesis by

Raimo Jaakko Hakkinen

In Partial Fulfillment of the Requirements

For the Degree of

Doctor of Philosophy

California Institute of Technology

Pasadena, California

1954

ACKNOWLEDGMENTS

The author wishes to express his deep gratitude to Dr. H. W. Liepmann. This research would not have been possible without his guidance and constant encouragement.

William Willmarth, George Skinner, K. Krishnamurty, Jan deBruyn and other members of the Transonic Group assisted in carrying out the experiments and through valuable discussions. Dr. Donald Coles made available results of his work at the Jet Propulsion Laboratory which is greatly appreciated.

The instruments used in the experiments could not have been built without the skill and cooperation of C. A. Bartsch and William Sublette of the Aeronautics Machine Shop.

The author wishes to thank Mrs. Beverley Cottingham for her excellent work and patience in the preparation of the manuscript.

ABSTRACT

The first part of this report describes the design and construction of a floating element skin friction balance. This instrument, which is essentially an improved version of Dhawan's balance, was applied to measurements of local skin friction in the turbulent boundary layer of a smooth flat plate at high subsonic Mach numbers and supersonic Mach numbers up to $M = 1.75$. The measured skin friction coefficients are consistent with the results of other investigations at subsonic and also at high supersonic speeds. The principal difficulties which exist in comparing skin friction coefficients at various Mach numbers are discussed.

The second part of this report describes the application of the Stanton tube technique to skin friction measurements near the base of a shock wave impinging upon a turbulent boundary layer. The floating element technique is inherently difficult to apply for skin friction measurements in non-uniform flow. Hence, a Stanton tube is calibrated by means of a floating element balance in a uniform flow field and then used to measure skin friction near the base of an impinging shock. Oblique shock waves were produced by two wedges of 2.5° and 4.6° semi-angles and a normal shock was generated by a choked channel. Skin friction and velocity profiles were obtained for these three cases at a free stream Mach number of 1.48.

TABLE OF CONTENTS

SYMBOLS

b	Width of Stanton tube
$C_f = \frac{\tau}{q}$	Local skin friction coefficient
h	Height of Stanton tube
h'	Distance from surface at which indication of Stanton tube corresponds to actual dynamic pressure
m	Ratio of trip mass flow per unit width of flat plate to mass flow defect of laminar boundary layer $(\rho_\infty U \delta^*)$
M	Mach number
p	Static pressure
p_τ	Pressure indicated by Stanton tube
$\tilde{p} = \frac{(p_\tau - p)\ p_w}{\mu_w^2}$	Calibration parameter of Stanton tube
$q = \rho_\infty U^2/2$	Free stream dynamic pressure
$R_x = U \rho_\infty x/\mu_\infty$ $R_y = U \rho_\infty y/\mu_\infty$ etc.	Reynolds number based on x, y, etc.
u	x-component of local velocity
U	Free stream velocity outside boundary layer
x	Streamwise coordinate
y	Coordinate normal to surface
α	Semi-angle of wedge
$\gamma = 1.4$	Ratio of specific heats
δ	Boundary layer, thickness

δ^*	Boundary layer *displacement* thickness
θ	Boundary layer momentum thickness
μ	Viscosity
ξ	Distance from point of intersection of shock with surface
ρ	Density
τ	Shear stress
$\tilde{\tau} = \frac{\tau_w \rho_w}{\mu_w^2}$	Calibration parameter of Stanton tube

Subscripts

h	Value at edge of Stanton tube
i	Incompressible flow
w	Value at solid surface
∞	Free stream value outside boundary layer
1	Value before shock wave interaction
$SUBS.$	Subsonic

PART 1

MEASUREMENTS OF TURBULENT SKIN FRICTION ON A FLAT PLATE AT TRANSONIC SPEEDS

I. INTRODUCTION

In recent years the importance of viscous effects in modern aero-dynamics has motivated a great number of both theoretical and experimental investigations in the field of boundary layer phenomena. For obvious reasons, particular attention has been given to the frictional forces introduced by these effects on the surfaces of bodies moving in a fluid. For the laminar boundary layer the theoretical evaluation of these forces has reached a well advanced stage, whereas for the turbulent boundary layer, the lack of knowledge of even some of the most basic properties of turbulent shear flows has prevented the development of quantitative theories. Thus, the skin friction associated with the turbulent boundary layer presents an important problem for experimental research.

There are many different ways of measuring skin friction (an exhaustive discussion of these is given in Ref. 1). However, it is clear that a direct measurement of the frictional force itself would be preferable to all others, provided that it could be performed with satisfactory accuracy. This technique was first used by Kempf in 1929 (Ref. 2) and then by Schultz-Grunow in about 1940 (Ref. 3). It was used again in 1950 by Dhawan (Ref. 1), who developed and demonstrated a satisfactory, relatively simple skin friction meter adaptable to high-speed

flow. Dhawan's work gave rise to a number of parallel investigations at different values of the flow parameters, with instruments based on the principles of his original device. Some of the results have already been published. Coles (Ref. 4), and Bradfield, DeCoursin, and Blumer (Ref. 5), have dealt with flat plates at Mach numbers from 2 to 5, and with axially symmetric configurations, respectively.

While Dhawan was able to obtain reliable measurements of subsonic skin friction on a flat plate with his original instrument, he encountered difficulties in extending his experiments to the supersonic range in the GALCIT 4" x 10" Transonic Wind Tunnel. The present investigation was undertaken in order to remedy this situation and to develop an instrument capable of reliable measurements of skin friction at supersonic speeds, even under the restrictions imposed by the size and characteristics of the existing facilities.

In the course of the investigation it was realized that problems of a more fundamental nature than the limitations of geometrical size or the establishing of satisfactory flow conditions were involved in the measurements and in their interpretation. The lack of knowledge about the proper definition of an "origin", that is, of an absolute streamwise Reynolds number scale of a turbulent boundary layer, makes it difficult to find a satisfactory way of comparing skin friction coefficients of low and high-speed turbulent boundary layers in a unique manner. This problem, which is of major importance at the Reynolds numbers obtained in the present experiments (approximately 10^6, based on the distance between leading edge and point of measurement), is discussed in detail in this report. A great deal of effort has been expended in

studying the characteristics of transition observed in the experiments as well as in the effects of various tripping devices.

In addition, one of the purposes of the present investigation was to develop an absolute instrument for use as a calibration device for other means of measuring skin friction currently under development at GALCIT. Results of one such application of the apparatus are described in the second part of the present report.

The project was conducted under the sponsorship and with the financial assistance of the National Advisory Committee for Aeronautics.

II. INSTRUMENTATION AND GENERAL TECHNIQUE FOR MEASUREMENTS OF LOCAL SKIN FRICTION

The skin friction meter used in the current investigation is a direct development of the original Dhawan instrument (Ref. 1) and differs only in structural details. (Figs. 1, 2, and 3 show the instrument with modifications for the supersonic experiments; in the subsonic experiments the leading edge was 1.2 cm. closer to the measuring element and no trip air holes existed.) The skin friction force acts on an elastically supported floating element in the plane of the flat plate and causes a streamwise deflection of this element. The displacement creates an electric signal which can easily be interpreted in terms of the skin friction force.

The flat plate was placed horizontally in the test section, approximately halfway between the ceiling and the floor, and fastened to the test section side windows at four points (Fig. 3). All structural members of the mechanism were attached directly to the plate and housed within a sealed windshield. The instrument forms a compact unit which can be completely assembled and calibrated outside the tunnel, thus permitting a very simple and quick installation. The angle of incidence of the flow over the instrument can be adjusted by rotating the windows, and the streamwise position of the instrument can be changed by interchanging the removable side wall panels of the test section. By means of these adjustments the conditions of non-uniform flow, which had seriously interfered with the preliminary measurements of Ref. (1) in the same tunnel, were eliminated and pressure

distributions within $\Delta p/q = \pm 0.02$ were realized throughout the whole range of experiments.

1. Force Sensing System

A Schaevitz 040-L variable differential transformer was used as the displacement sensitive element. The electrical circuit (Fig. 4) is similar to the one described in Ref. (1). A Hewlett-Packard 200B oscillator was used as the power supply. The output circuit was equalized by a 25,000 ohm potentiometer. Input and output voltages were read on Hewlett-Packard vacuum tube voltmeters. Input frequency was 20 KC in all cases and the input voltage ranged from 4 to 10 volts r.m.s. The sensitivity of the instrument is determined by the flexure links. At subsonic speeds flexure links made of 0.0045" x 1/16" steel strip gave, at 4 volts input, a sensitivity of 6.05 volts/cm. or 0.144 volts/gram. At supersonic speeds the flexure linkage was made more rigid (0.006" x 1/16") in order to withstand shock loads. A sensitivity of 15.1 volts/cm. or 0.129 volts/gram resulted at 10 volts input. In both cases a small dashpot filled with 1,000 centistokes silicone fluid provided adequate damping. Calibration was carried out by hanging weights directly on the moving part of the mechanism with a single-fibre nylon string passing over an aluminum pulley on jewel bearings. Calibration curves used for the present results are given in Fig. 5. The repeatability of calibration was within $\pm$ 1 percent of the readings recorded in the high-subsonic and supersonic regions. This performance, together with observations of zero shift discussed in the next section, led to the conclusion that the added complexities of a null-

reading system or of a more elaborate electrical circuit would not be justified. The possible, and by no means guaranteed, improvements in accuracy would be small because of the difficulties imposed by the small size of the instrument.

2. Effects of Thermal and Elastic Deformations

The most serious problem in the design of the instrument was the elimination of zero shift, which was due mainly to thermal deformation of the structural parts of the instrument and, to some extent, also of the wind tunnel. After a considerable amount of experimentation a satisfactory solution was obtained. It is believed that a homogeneous structure completely symmetrical about the point of measurement is essential to the success of this type of instrument. The importance of thermal deformations is apparent from the fact that the total travel of the measuring element, corresponding to the maximum measurable force, was 0.012 cm. in the subsonic experiments and 0.005 cm. in the supersonic ones. There was no noticeable thermal effect on the electrical equipment, as was shown by calibrations over the range of surface temperatures occurring in the tunnel. A Western Electric Thermistor was mounted in the plate near the force element in order to ascertain that thermal equilibrium had been reached before measurements were taken.

In order to eliminate all possible effects arising from the operation of the tunnel (thermal, elastic, vibrational), experiments were run at each flow condition with the element isolated from the flow by means of a sealed shield which could easily be attached to the plate. The

results of these experiments showed that no zero-shift correction was necessary at subsonic speeds, where the surface of the instrument was approximately at room temperature. In the supersonic experiments the stagnation temperature had to be raised to 55-65°C in order to avoid condensation of water vapor in the test section. A zero shift of approximately one percent of the force at these speeds was then observed during the operation of the tunnel. It was, however, found to be repeatable if the tunnel was warmed up before a measurement was made and if the duration of the run was not longer than five or ten minutes. With the same precautions, the initial and final zero readings taken immediately before and after an experiment were found to be in agreement within the accuracy of the calibration of the instrument.

In the experiments of Dhawan, the measured skin friction was strongly influenced by rate of change of stagnation temperature, this being tentatively attributed to the effect of heat transfer on the skin friction. The magnitude of this effect was up to 50 percent of the surface shear stress in a direction opposite to theoretical predictions. In the development of the present instrument, a preliminary model showed the same behavior, which, it was definitely established, was caused by transient thermal deformations of the instrument structure. The final instrument gave, under the same conditions, an effect of only a few percent in the direction predicted by theory. It cannot be concluded, however, that the remaining small effect is entirely due to heat transfer. Reliable information on this phenomenon should be obtained by instruments designed specifically for this purpose.

3. Pressure Distributions

Pressure distributions were measured by means of six pressure orifices on the plate. In addition, the gap around the element and the outlets for trip air at supersonic speeds were used as pressure orifices. In the adjustment of the pressure field, great care was taken to obtain not only a satisfactory over-all distribution but also as nearly a zero pressure gradient as possible around the element. The importance of this procedure is evident from the fact that the presence of pressure disturbances has a four-way influence on the skin friction values measured by the floating element, through:

1. Changes upstream in the boundary layer.
2. Direct local effect of pressure gradient on the velocity profile.
3. Pressure forces acting on the sides of the floating element.
4. Disturbances of velocity profile caused by air flow around the floating element due to different static pressures in the gaps.

Some of these effects, especially the pressure forces described in (3), can easily create errors of the same order of magnitude as the shear force itself. However, it is clear that the total error will vary from case to case. Hence, it would be extremely difficult to establish the values of the proper corrections, both because of the lack of knowledge of the phenomena involved and because of the difficulties associated with the accurate measurements of the pressure gradient itself. Therefore, instead of trying to determine the corrections theoretically or experimentally, it was decided to minimize the pressure force effect by designing the gaps so that they expand inward. It was also decided

to make several measurements at approximately the same Mach number, introducing slight changes in the pressure distribution by varying the shape of the flexible nozzle. This technique was applied to the supersonic measurements and the results are discussed in detail in Section V. Although the measurements necessarily show some scatter, it is believed that their average values are relatively good indications of the shear stresses which would be obtained under ideal pressure distributions on the flat plate.

The Mach number given for each flow configuration was based on static pressure measured at the element.

4. Effect of Gaps Around the Floating Element

In the interpretation of the results a new problem arose with regard to the proper reference area of the measuring element. It is evident that if the measured force is simply divided by the actual area of the element, the resulting shear stress will be slightly high since the effects of slip of the surface air over the gap, as well as the shear exerted on the air in the gap, will have to appear as increased skin friction around the gap and as pressure differences on the sides of the gap, respectively. Both of these effects influence the measured force. The only available information on this problem is contained in Refs. (6) and (7) (both are quoted in the more readily available Ref. (8)). However, the gaps investigated in these experiments are relatively large, amounting to one-half or more of the total apparent boundary layer thickness, whereas the gaps of the present investigation are only of the order of a few percent of the apparent total thickness. Therefore, it is believed

that the effect of the gaps in the present case can be no larger than the effects found in the experiments referred to above, where the drag increment was found to be approximately the area multiplied by twice the undisturbed shear stress. On the other hand, it is not conceivable that the drag of a smooth surface would be decreased by gap-like disturbances. Hence an upper and lower limit is established for the force increment due to the gaps.

It is still important to know how this force increment is distributed between the moving element and the surrounding plate. As the element experiences the downstream effect of one gap and the upstream effect of the other it may be assumed that it experiences half the force increment, although strictly speaking the change in size of the upstream and downstream gaps as the element moves should be taken into account. In the present instrument the total front and rear gap area is 11 percent of the element area. Half of this, multiplied by the shear stress gives the lower limit of the force on the element due to the gaps, and multiplied by twice the shear stress gives the upper limit. For computation of shear stress, then, the "effective element area" should be taken as from 5-1/2 percent to 11 percent greater than the actual area. In the present results 8-1/4 percent was used as a working average.

No correction has been made for the possible effects of the gaps at the ends of the element, and it is believed that the overall systematic error due to the gaps lies within $\pm$ 3 percent.

It should be emphasized that the above reasoning and the adopted procedure are crude approximations. Evidently, however, any more

accurate information on the problem would have to be obtained by careful experiment. This would be a major project in itself, especially in view of the lack of definite knowledge of the proper parameters to use as variables in studying the effect. It should also be emphasized that the large magnitude of the gap effects in the present case is entirely due to the small size of the instrument. In larger instruments the gap area can be made very small compared to that of the element, and the effects reduced to negligible amounts.

5. Accuracy of the Skin Friction Measurements

With $\pm$ 1 percent repeatability of calibration and $\pm$ 3 percent probable magnitude of the gap effect, measurements of the surface shear stress, performed in a zero pressure gradient, can be obtained with a maximum error of $\pm$ 5 percent. In actual experiments, and in their evaluation, additional errors are introduced into the skin friction coefficients by inaccuracies in the determination of flow parameters (dynamic pressure and Reynolds number)and by pressure disturbances in the free stream. These errors depend on the individual flow configurations and are partly reflected in the scatter of the measured values. The principal systematic uncertainty in this group is connected with the definition of proper reference Reynolds numbers and is discussed in detail in the next section.

III. REMARKS ON TURBULENT BOUNDARY LAYERS AT LOW REYNOLDS NUMBERS

The results of theoretical and experimental investigations of the compressibility effect on turbulent skin friction have been generally expressed in the form of the ratio of compressible to incompressible skin friction coefficients for identical streamwise Reynolds numbers. This procedure has been satisfactory at the high Reynolds numbers of most of the previous experimental data. However, some doubts have arisen regarding the validity of the method for interpretation of the current experiments, which were performed at relatively low Reynolds numbers. The difficulty in question is a direct consequence of a certain arbitrariness in the definition of the Reynolds number as a characteristic quantity of the turbulent boundary layer. It is the purpose of this section to discuss the problem in detail and to propose suitable procedures for analyzing the results of the present investigation.

1. Transition from Laminar to Turbulent Flow

If we consider a smooth flat plate large enough to develop transition into turbulent flow the general picture is the following:

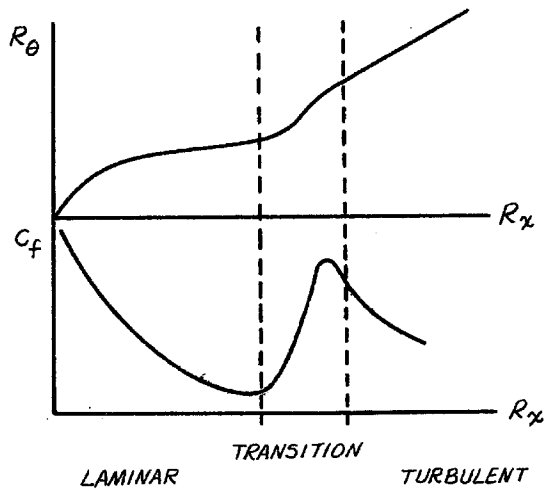

$$c_f = \frac{\tau_w}{q} = 2\,\frac{dR_\theta}{dR_x}$$

$$R_\theta = \int_0^\infty \frac{\rho u}{\rho_\infty U}\left(1 - \frac{u}{U}\right) dR_y$$

$$= \frac{1}{2}\int_0^{R_x} c_f\, dR_x'$$

$$R_y = \frac{\rho_\infty U y}{\mu_\infty}$$

It has been verified experimentally that laminar flow is well described by the existing theories. Very little is known about transition quantitatively, and it has been demonstrated that the characteristics differ from case to case. While it would be reasonable to expect that (at a certain Mach number) transition on flat plates of sufficient smoothness would occur for the same R_x (based on distance from the leading edge) and would bear a certain relation to R_θ and c_f, it should be noted that, under actual physical conditions, disturbing effects always occur and in many cases are even deliberately introduced, often in a crude manner, to induce transition. Thus, in reality, the position and structure of transition do not follow any specified law, consequently we cannot expect to have a well-defined starting point for the turbulent boundary layer in terms of R_x, R_θ, or c_f.

2. The Fully Developed Turbulent Boundary Layer

Downstream of the transition region, a relation between c_f and R_θ has been experimentally shown to exist for incompressible boundary layers (there is an extensive discussion of available data in Ref. 9). Whether this relation is truly independent of secondary effects, such as the free stream turbulence level, has not been definitely shown, however, it is believed to be sufficiently well founded to be used under ordinary conditions. Further, there appears to be no evidence against an extension to compressible flows, although the experimental support cannot yet be considered sufficient. In the following discussion it is assumed that, downstream of the transition region on a flat plate, a relation of sufficient practical accuracy exists connecting c_f, R_θ, and

M. Where this relation holds the turbulent boundary layer is described as "fully developed".

3. The Reynolds Number of a Turbulent Boundary Layer

Since $c_f = 2(dR_\theta/dR_x)$, the relation assumed above connects R_x with c_f, R_θ, and M, except for an arbitrary constant which requires the introduction of one further condition. Although not always explicitly pointed out, the same situation has also occurred in theoretical considerations. In von Kármán's original incompressible results (Refs. 10 and 11) and Coles' re-evaluation of them (Ref. 9) for example, a condition that $R_x = 0$ when $c_f = \infty$ has been applied, although the "point of origin" thus defined does not have any counterpart in a physical configuration. In experimental work, the data have either been fitted to an assumed theoretical law (Refs. 12 and 13), or based on a length such as that from the leading edge (Refs. 1, 2, 3 and a large number of other investigations), tripping device, shear stress peak in the transition region (Ref. 9), etc. These methods of defining point of origin need not be such as to permit a comparison of results in a unique manner. At least for the present, there seems to be no clear way out of this difficulty.

It is fortunate that the combined laminar and transition regions seem to be limited in size to a Reynolds number from the leading edge of the order of 10^6 (at least up to moderate supersonic Mach numbers). Thus, by working at sufficiently high Reynolds numbers a large part of the distance between the station of measurement and the leading edge is covered by the fully developed turbulent boundary layer. With

increasing Reynolds number, we can then expect to be able to establish an asymptotically improving description of the boundary layer characteristics in terms of a Reynolds number based on any of the physical lengths mentioned above. The contribution of the laminar and transition regions to R_θ and R_x becomes relatively so small that differences in position of transition cannot influence the results to a significant extent. That this kind of behavior is actually true has been demonstrated by a large number of experiments with widely varying conditions near the leading edge. (Graphical summaries are given in, for example, Refs. 14 and 15.) As a practical procedure one could use the distance from the leading edge of a flat plate as the basis for Reynolds number whenever the ratio of the distances of the point of measurement and the end of the transition region, from the leading edge, is large. Thus, for incompressible flow with a natural transition region somewhere near $R_x = 10^6$ (from the leading edge), one could expect the measurements to be in reasonable agreement at $R_x > 10^7$. This is, in fact, what has been observed.

The fact that some experiments with artificial tripping (for example, Ref. 1), where the Reynolds number has been based on the distance from the leading edge or tripping device, follow von Kármán's law closely down to about 2×10^5 is merely a reflection of the fact that in terms of von Kármán's law the origin ($R_x = 0$) of the fully developed layer falls close to the normally occurring locations of the transition zone. It should be emphasized, however, that in a rigorous sense the Reynolds number used in the description of these experiments has little significance. The only correct way of identifying a fully developed

turbulent boundary layer in terms of a suitably defined streamwise Reynolds number is by means of the local value of c_f, or R_θ.

For the compressible turbulent boundary layer, we are, at present, not even in possession of a theoretical relationship comparable to von Kármán's incompressible law. Several attempts have been made in this direction (Refs. 12, 16, 17, 18, and 19; see summary in Ref. 9) but none of them has the support of sufficient experimental evidence. Furthermore, unless a theoretical law were a direct extension of von Kármán's compressible law, it obviously would not need to have any connection with the definition of Reynolds number in that case. Many of the relations referred to above are, in fact, attempts at such an extension, but their theoretical foundations differ from case to case and are often artificial. It is believed that the present stage of knowledge does not allow a meaningful definition of Reynolds number to be established, except at the larger Reynolds numbers where the leading edge, tripping device or some characteristic of transition can again be used as a reasonable basis in the same manner as in the incompressible case. That the compressible fully developed turbulent boundary layer actually follows a similar asymptotic relation has been demonstrated by Coles (Refs. 4 and 9). At the low Reynolds numbers it is evident, however, that in a rigorous sense all one can hope to obtain from an experimental investigation of a compressible turbulent boundary layer is the supposed relationship between R_θ, c_f, and M.

4. Comparison of Compressible and Incompressible Boundary Layers at Low Reynolds Numbers

To attach an approximate streamwise Reynolds number to

measurements performed in compressible flow in the low Reynolds number range one would, for instance, be tempted to assume a point of origin close to the transition zone, as in the incompressible case. Despite the fact that in compressible flow both the laminar and the transition regions are different from incompressible flow (as regards both the streamwise extent, in terms of Reynolds number, and the structure of the regions, in terms of R_θ and c_f), Coles has found the use of peak shear, as an origin for Reynolds number, to give a reasonably good description of his experimental results. The application of the peak shear criterion to the results of the present investigation is discussed in Section V.

An apparent way out of the difficulty would be to compare the skin friction coefficients, not at the same R_x, but at the same R_θ. This would leave no arbitrariness in the evaluation of experimental results. Some difficulty can be seen, however, in the fact that certain values of R_θ would probably not fall within the physically realizable fully developed turbulent region at all Mach numbers. Neither does this concept of compressibility effect bear as direct a connection to physical configurations as the comparison in terms of Reynolds numbers based on some measurable streamwise distance.

The highest Reynolds numbers (measured from the leading edge) occurring in the present experiments were about 1.2×10^6. All data thus fall in the range where the streamwise Reynolds number cannot be defined accurately. In view of the above discussion it was decided to use the following methods in the analysis:

Subsonic Measurements: Reynolds number based on distance

between leading edge (or trip) and the point of measurement.

Supersonic Measurements: (i) Reynolds number based on distance between observed shear peak in transition region and point of measurement. (ii) Reynolds number based on momentum thickness computed from measured velocity profile.

Since incompressible results, theoretical or experimental, based on the same criteria are not available, except in the case of momentum thickness, the relations of von Kármán (Ref. 11) and of Coles (Ref. 9) are used instead.

IV. MEASUREMENTS IN SUBSONIC FLOW

Although the main aim of the present experiments was to investigate turbulent skin friction at the supersonic end of the transonic regime, it was decided to obtain a few subsonic measurements in order to compare them with existing results. Several Mach numbers, beginning at 0.18, were covered; the Reynolds numbers ranged from 0.33×10^6 to 1.20×10^6.

1. Experimental Technique

In the subsonic experiments the instrument was placed directly above the flexible nozzle, which was used to great advantage in adjusting the pressure gradient on the flat plate. The pressure distributions are shown in Fig. 7. Although the measurement at $M = 0.97$ is not satisfactory, due to a supersonic zone at the leading edge, it is included as an illustration of conditions obtainable close to sonic speed.

At subsonic speeds the expansion of the flow around the sharp, half-wedge leading edge has some destabilizing effect on the boundary layer. However, it was concluded from preliminary experiments that this effect alone was not sufficient to create a satisfactory turbulent flow on the flat plate. Several additional tripping devices were tried until, finally, a three-dimensional rake cemented on the leading edge was adopted. The final trip consisted of 0.02 cm. diameter pins about 0.3 cm. long mounted 0.3 cm. apart and swept back about 45°. Variations of this rake, involving slightly different pin dimensions and mountings, had no additional influence on the local skin friction

measured at the element. Fig. 6 shows the effects of various tripping devices.

The Reynolds number used in the evaluation of these measurements was based on the distance between the leading edge (or trip) and the measuring element, as was done in Dhawan's experiments. A closer investigation of the transition region was not attempted in the subsonic measurements.

2. Discussion of Results

The measured local skin friction coefficients are presented in Table I and Fig. 8. Incompressible references curves are the original von Karman-Kempf result (Ref. 11), a proposed modification by Dhawan, and the most recent re-evaluation of available data by Coles.

The results show a scatter of approximately $\pm$ 5 percent. This scatter is believed to be largely due to the effect of free stream pressure disturbances. Referring to the estimated $\pm$ 5 percent uncertainty of the shear stress measurement and the indeterminacy of the Reynolds number, it is not considered worthwhile to make a more detailed analysis of the accuracy of the subsonic experiments.

It can be concluded, however, that the measurements are in substantial agreement with previous evidence, especially with Dhawan's work. That compressibility slightly decreases the skin friction at the higher subsonic Mach numbers is clearly demonstrated.

V. MEASUREMENTS IN SUPERSONIC FLOW

The supersonic experiments were performed at two Mach numbers, about 1.50 and 1.75. The Reynolds number, based on the distance between leading edge and measuring element, was approximately 10^6 in both cases.

Previous experimental information on turbulent skin friction at these speeds is not very extensive, and on local skin friction values it is extremely scarce. No direct force measurements, other than Dhawan's preliminary ones, have been reported for flat plates. Other results could be obtained by differentiation of momentum thickness distributions reported in several references, but this procedure is very inaccurate.

At Mach numbers above 2, Coles (Refs. 4 and 9) has recently obtained extensive measurements of local skin friction by the floating element technique. Cope (Ref. 20) has reported some local measurements at M = 2.5 by means of a Stanton tube, but the use of calibration obtained in low-speed flow renders his results doubtful.

In the absence of adequate theoretical work, the present experiments can be compared with the behavior interpolated from existing incompressible data and Coles' measurements at higher Mach numbers.

1. Experimental Technique

In the subsonic experiments, the instrument was placed in the test rhombus of the wind tunnel. Mach number and pressure distribution on the flat plate were controlled by the flexible nozzle mechanism. Due to the large streamwise extent of the model and the limited amount

of control of the nozzle shape, it proved exceedingly laborious to establish satisfactory flow conditions, a difficulty experienced by Dhawan in his preliminary measurements. However, with the greater variety of installations allowed by the present design, useful configurations were found at Mach numbers around 1.50 and 1.75. At lower supersonic Mach numbers, a detached shock wave from the housing of the force sensing mechanism interfered with the flow ahead of the leading edge and no measurements were attempted in this range. Several measurements were taken at each Mach number with slight differences in pressure distributions. Typical pressure distributions are presented in Fig. 9.

Since the Reynolds number per unit length available in the GALCIT Transonic Wind Tunnel is about the same for high-subsonic and supersonic speeds, measurements were first made using the same trip rake as in the subsonic experiments described in the preceding section. These measurements yielded values so much below those expected that a closer investigation of the transition region was deemed necessary. For this purpose a variable trip, based on the principle of air injection described in Ref. 21, was devised. This trip consisted of a row of 0.05 cm. holes close to the leading edge through which air jets were directed into the boundary layer. The mass flow of the trip air was measured by means of a Fischer and Porter floating-ball type flow meter. The modified flat plate is illustrated in Fig. 2.

For an investigation of the transition region, a slit-like total head tube was employed which could be moved along the flat plate surface within the limitations of the traversing mechanism. Although its opening was only about 0.02 cm. wide, it was too large to be used as a

Stanton tube for quantitative measurements of shear. However, it is believed that the probe still provided a qualitative indication of the actual surface shear stress.

Some velocity profile measurements were made using another slit-like total head probe similar to the one used in the transition investigation. The probe position was observed by means of a cathetometer.

2. Effect of Variable Tripping on Transition and Local Skin Friction

Surface total head surveys of the supersonic configurations are presented in Figs. 10 and 12. The vertical coordinate $\sqrt{\frac{p_t - p}{q}}$ was chosen because it would be proportional to the local skin friction coefficient, if the probe were completely within the uniform velocity gradient close to the wall, and if there were no viscous and compressibility corrections to the "average" pressure read by it.

The parameter varied to obtain the curves in Figs. 10 and 12 is the ratio of trip air mass flow per unit width of the plate to the mass flow defect ($\rho_\infty U \delta^*$) of the laminar boundary layer at the location of the trip. Computation of the mass flow defect was based on Ref. 22, where the following formula is given for the displacement thickness of a compressible laminar boundary layer

$$\delta^* = \delta_i^* \left[1 + \frac{\gamma - 1}{2} \left(1 + \frac{\theta_i}{\delta_i^*} \right) M^2 \right]$$

Figs. 11 and 13 present typical variations of the skin friction measured at the floating element when the trip mass flow was varied. At both Mach numbers the skin friction decreased with increasing mass flow from a peak value (when the peak shear of the transition zone

passed over the element) to a small shelf-like constant region followed by further slow decrease. The skin friction measurements were taken normally in the shelf-like region. Some values based on the slow decrease region were obtained at M = 1.75, although it is possible that the corresponding location of peak shear was influenced by local effects due to air jets. Some experiments, carried out with a trip hole spacing half that described in Fig. 2, did not show any change in the transition characteristics.

It should be noted that the natural transition at M = 1.75 was just beginning at the element, corresponding to a Reynolds number of 10^6, whereas at M = 1.5, laminar flow could not be maintained beyond about $R_x = 3 \times 10^5$. This corroborates other experimental evidence of the stabilizing effect of compressibility which has been reported by several investigators (a recent survey of the problem has been presented in Ref. 23). A related phenomenon may be the fact that the distances between the trip jets and the shear peaks, for a given trip air mass flow, were noticeably larger at M = 1.75 than at M = 1.5.

The behavior of transition shown in the figures referred to in this section was not quite repeatable, probably owing to variable deposits of dust on the plate. The results are, therefore, not to be considered directly transferable to other experimental configurations.

3. Discussion of Results in Terms of Streamwise Reynolds Number

The measurements of supersonic skin friction in terms of Reynolds number based on distance from location of peak shear are presented in Table II and Fig. 16.

In each range, the measured points were used to obtain values of c_f/c_{f_i} at one Mach number in the range by extrapolating from each point, using the slope of von Kármán's theoretical curve (Ref. 16). These values were then averaged. In view of the small shifts involved, this approximation is believed to introduce negligible error. The scatter before averaging was $\pm$ 3 percent. Since the distribution was clearly non-Gaussian, error theory could not properly be applied and the probable error of less than $\pm$ 1 percent which it gives is no doubt too small.

The scatter is thought to be due to disturbances in the free stream pressure field and difficulties in locating the peak shear, rather than errors in the measurement of shear stress itself. It should therefore be considered separately from the more or less systematic shear stress measurement error of $\pm$ 5 percent in the measurements under ideal conditions. The additional uncertainty arising from the indeterminacy of the compressible and incompressible Reynolds numbers is connected with the validity of the whole procedure of evaluation of the results, and a reliable estimate of these errors cannot be attempted. Therefore, a discussion of accuracy beyond that given for the shear stress measurement and the scatter of the present results is believed to be pointless.

It should be noted that according to von Kármán's estimate (Ref. 16) the c_f/c_{f_i} value at a certain Mach number should decrease slightly with increasing Reynolds number. In view of this possibility the average results in terms of streamwise Reynolds number indicate a good agreement with behavior interpolated from incompressible results and those of Coles at higher Mach number.

4. Discussion of Results in Terms of Momentum Thickness

The results obtained in terms of dimensionless momentum thickness are presented in Table III and Fig. 17. Velocity profiles used in the evaluation of the momentum thickness are given in Figs. 14 and 15.

These results involve too few measurements to permit an accuracy estimate on the basis of scatter. The momentum thicknesses were determined by graphical integration from velocity profiles, which in turn were computed from the total head readings applying the constant energy assumption. Errors arise from this procedure as well as from inaccuracies of the cathetometer readings. No velocity gradient correction has been made to the total-head tube position in view of the recent experimental results obtained in supersonic turbulent boundary layers (Refs. 13 and 14). Without attempting to estimate the total maximum error numerically, it is believed to be of the order of several percent.

The results indicate the decrease of skin friction at these Mach numbers to be slightly less than that obtained when streamwise Reynolds number is used. It should be noted that the $M = 1.75$ values seem high, although within experimental accuracy, compared with the $M = 1.5$ results. This may be an indication that the local effects of transition had not yet completely disappeared from the boundary layer at the element, which is quite possible in view of the lower Reynolds numbers obtained at this speed.

VI. CONCLUSIONS

The relatively small and compact GALCIT direct skin friction meter has been further developed and applied to the investigation of high-speed turbulent boundary layers on a flat plate at Mach numbers up to 1.75.

Accuracy within ± 5 percent can be obtained under ideal flow conditions. This is capable of substantial improvement in large instruments, or with more information on the effects of gaps around the measuring element.

In the range of the present experiments, the lack of knowledge of the proper definition of an absolute streamwise Reynolds number for turbulent boundary layers introduces a fundamental difficulty into a comparison between compressible and incompressible skin friction at the same Reynolds number, and necessitates the use of approximate methods for evaluation of the results. At Mach numbers 1.5 and 1.75, a decrease of skin friction coefficient from the incompressible value (based on Coles' relation) of approximately 10 percent was observed.

A comparison of the measured skin friction coefficients with incompressible values at the same dimensionless momentum thickness showed a slightly smaller compressibility effect.

PART 2

MEASUREMENTS OF SKIN FRICTION IN A TURBULENT BOUNDARY LAYER WITH SHOCK WAVE INTERACTION

VII. INTRODUCTION

The interaction of a boundary layer with a shock wave is one of the more complicated problems of present day fluid mechanics. Contrary to the practice at low speeds, the division of the flow field into non-viscous flow, responsible for pressure forces, and boundary layer regions, responsible for skin friction, is not clear-cut. The strong pressure gradients at the shock wave have an effect on the boundary layer which alters its characteristics over a small distance sufficiently to cause changes in the outer flow field. In some cases the effect on the boundary layer is very pronounced, leading to such phenomena as separation and back flow within the boundary layer.

The general qualitative features of the problem are fairly well known from several experimental investigations (Refs. 25, 26, 27, 28, 29, 30, and 31). A considerable amount of theoretical literature is also available on the subject. It is not, however, the purpose of the present report to discuss the merits of the various theories which, due to the complexity of the problem, are still at a more or less qualitative stage. It is believed that at present more experimental information is needed in order to obtain guidance on suitable approximations for further analytical work. This is especially true in regard to the turbulent boundary layer which is not well understood even under undisturbed

flat plate conditions.

One of the important details of shock-wave boundary-layer interaction is the effect on skin friction. The qualitative theoretical and experimental work so far has indicated that there should be a tendency for the skin friction to decrease in the interaction region, and, with sufficiently strong pressure rise through the shock wave, local separation may occur.

Only three attempts are known to have been made to obtain quantitative values of the skin friction in the interaction region experimentally. Ackeret, Feldmann and Rott (Ref. 25) in 1947 tried to estimate the distribution of skin friction in an interaction zone from observed velocity profiles, applying an integral form of the equations of motion. This method is, however, inaccurate since it involves differentiation of momentum thickness distributions and taking differences between large numbers. Fage and Sargent (Ref. 27), as well as Cope (Ref. 20), applied the Stanton tube technique (a slit-like total head tube at the solid surface) for measurements of skin friction. Their calibrations were made at subsonic speeds; as will be shown later, it is not reliable to extend a subsonic calibration of a Stanton tube to supersonic speeds. Therefore, the previous experimental evidence on the problem of skin friction distribution in a shock-wave boundary-layer interaction region is of a qualitative nature.

With the design of a direct skin friction meter for high speed flow at GALCIT by Dhawan in 1950 (Ref. 1), a new possibility was made available for the measurement of skin friction. It soon became apparent, however, that the floating element technique was best adapted to

conditions with zero pressure gradient across the element. In the presence of large pressure gradients, pressure differential between the gaps upstream and downstream of the floating element would give rise to forces many times the skin friction force acting on the element. This difficulty together with other possible errors was discussed briefly in Part 1. The floating element could possibly be calibrated for use in small pressure gradients, but for gradients such as those occurring near shock wave, the calibration would probably prove very difficult indeed.

The fact that the streamwise extent of a practical floating element is of the same order as that of the shock-wave boundary-layer interaction zone, means that no real "point" measurements could be obtained.

However, the floating element can be used as a reference instrument against which one can calibrate some other instrument more suitable for use in strong pressure gradients. Two such instruments have been considered: A gage utilizing the relation between local heat transfer and local skin friction, and the Stanton tube. The results of an investigation of the heat transfer method will appear in a forthcoming GALCIT report. It is the purpose of the present paper to describe the results of an application of the Stanton-tube floating-element combination to the problem of shock-wave turbulent boundary-layer interaction.

VIII. INSTRUMENTATION AND CALIBRATION PROCEDURE

The flat plate with the direct skin friction meter described in Part 1 of this report was used. On this plate, a small Stanton tube was installed to one side of the floating element. A wedge airfoil mounted on the traversing mechanism of the tunnel could be moved so that the shock wave generated by the wedge impinged on the flat plate at any desired distance upstream or downstream of the Stanton tube. Static pressure was observed with an orifice between the floating element and the Stanton tube. A Western Electric Thermistor mounted in the flat plate measured surface temperature for the evaluation of surface viscosity and density. A total head probe flatened to 0.02 cm. thickness was used for observation of velocity distribution in the boundary layer.

Fig. 18 shows the general installation of the test equipment in the GALCIT 4" x 10" Transonic Wind Tunnel.

1. General Characteristics of the Stanton Tube

The Stanton tube (surface total head, "half-pitot") was invented and employed for skin friction measurements by Stanton in England in about 1920 (Ref. 32). Subsequently it was applied to the determination of skin friction on airfoil shapes by Fage and Falkner in 1930 (Ref. 33). In 1938 Taylor (Ref. 34) collected previous data, and adding some results of his own, showed that all calibrations could be reasonably well described by a single relation between dimensionless parameters

h/h' and $\tau_w \rho_w h^2/\mu_w^2$, where h is the height of the tube and h' the distance from surface to point where velocity corresponding to dynamic pressure observed by the tube would occur. This relation can also be expressed in a form more convenient for our purposes:

$$\frac{\Delta p\ \rho_w h^2}{\mu_w^2} = f_n\left(\frac{\tau_w\ \rho_w\ h^2}{\mu_w^2}\right)$$

where Δp is the difference between the tube pressure and the local static pressure. Introducing parameters $\tilde{p} = \Delta p\, \rho_w/\mu_w^2$ and $\tilde{\tau} = \tau_w \rho_w/\mu_w^2$ we may write

$$\tilde{p} h^2 = f_n(\tilde{\tau} h^2)$$

Taylor further showed that for small values of $\tilde{\tau} h^2$ the pressure increase Δp is a linear function of the shear stress τ_w

$$\Delta p = \text{CONST.}\ \tau_w$$

or also

$$\tilde{p} h^2 = \text{CONST.}\ (\tilde{\tau} h^2)$$

The mechanism responsible for the pressure increase is then essentially a viscous one without significant inertia effects (Stokes flow). For higher values of $\tilde{\tau} h^2$ the relation gradually approaches a square law

$$\tilde{p} h^2 = \text{CONST.}\ (\tilde{\tau} h^2)^2$$

This form would result directly from averaging the dynamic pressure of a linear velocity distribution across the mouth of the tube and thus corresponds to the limiting case of negligible viscous effects. A more detailed discussion of the calibration relation and its form in the limiting cases is given in the Appendix.

Fage and Sargent in 1947 calibrated their Stanton tube in a

subsonic boundary layer, calculating their reference skin friction values from an approximate momentum equation. Cope in 1951 did not even calibrate his particular tube but directly applied Taylor's universal low-speed relation to an investigation at M = 2.5. In the present investigation it was for the first time possible to obtain reference values from absolute measurements of surface shear stress at the same flow condition. Even this method of calibration is, of course, still restricted to zero pressure gradients. The application of the calibration to measurements in boundary layers with pressure gradients may still introduce some errors. It can be expected, however, that these errors would be less serious than in the case of the floating element. If the pressure difference over the width of a floating element is equal to the shear stress, the error from pressure forces in the gaps acting on the sides of the element would evidently be of the order of the skin friction force itself. In the case of a Stanton tube, the dimensions of the region within which the pressure rise observed by the tube is created are of the order of the height of the tube. Since this height can be made a small fraction of the streamwise extent of a floating element, and since the observed pressure rise generally is many times the value of the shear stress, the Stanton tube is likely to tolerate pressure gradients of a larger order of magnitude than the floating element without introducing serious errors to the measurements of skin friction. However, further experimental work, which was not feasible with the facilities available, would be desirable in order to establish more definitely the behavior of the Stanton tube in pressure gradients.

2. The Present Stanton Tube

The Stanton tube built for the present investigation has the following dimensions:

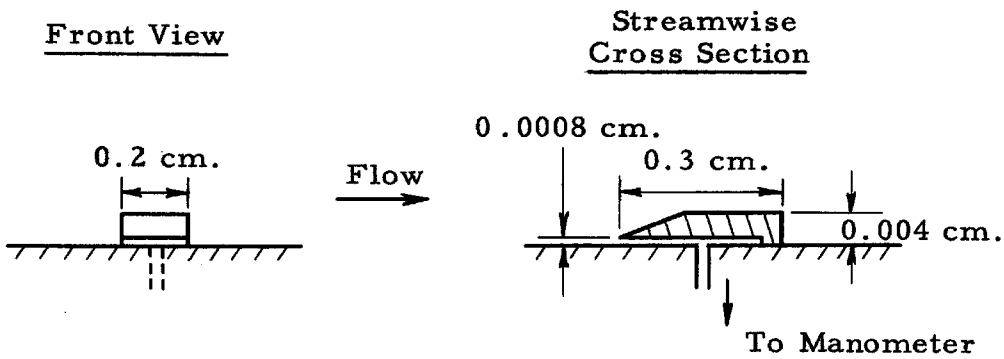

In order to keep the tube within the subsonic part of the boundary layer, the dimensions were made as small as practicable. The pressure difference between the tube and an adjacent static pressure orifice was measured by an alcohol manometer. Due to the slow response of the Stanton tube, a technique of bleeding air into or out of the manometer was developed; in this manner, the reading could be bracketed within a few percent in one or two minutes. The final reading was taken several minutes later after all other measurements were recorded. It may be noted that the pressure reading was very sensitive to changes in flow temperature, as might be expected from the form of the calibration parameters, and it was important to keep the temperature level constant during measurement.

3. Calibration

The calibration results obtained in subsonic flow are shown in Fig. 19. These results, which cover a range of Mach numbers from

approximately 0.2 to 0.9, are well described by a 5/3-power law connecting the pressure and shear parameters. This indicates that the mechanism responsible for the observed pressure rise is partly dynamic and partly viscous. In view of the difficulty of determining the effective height of the Stanton tube accurately, the parameters $\tilde{p}$ and $\tilde{\tau}$ used here do not include the tube height and therefore have the dimension cm.$^{-2}$. Since only one tube configuration was used in all experiments, this procedure is legitimate.

In supersonic flow, it proved difficult to establish satisfactory flow conditions in the GALCIT Transonic Wind Tunnel for reliable use of the floating element. The calibration had to be limited to essentially two Mach numbers only. Hence only a rather narrow range of the shear parameter could be covered. Even then the results showed considerable scatter which is believed to be due to the influence on the floating element of disturbances in the free stream. However, the pressure readings in supersonic flow were definitely higher than corresponding values in subsonic flow. As well as could be determined within the range and scatter of the observations (Fig. 20), the ratio of supersonic to subsonic pressure parameter followed a simple M^2 relation with sufficient accuracy. It does not seem possible to account for an effect of this magnitude by considering variations of density and viscosity in the boundary layer (see Appendix). It is therefore believed that the increase is caused by static pressure rise through shock waves generated in the supersonic part of the boundary layer by deflection of the flow over the Stanton tube.

The final formulae used for reduction of observed data were the following:

Subsonic

$$\tilde{\tau} \times 10^{-7} = 0.637 \left(\tilde{p} \times 10^{-8}\right)^{3/5}$$

Supersonic

$$\tilde{\tau} \times 10^{-7} = 0.637 \left(\frac{\tilde{p} \times 10^{-8}}{M^2}\right)^{3/5}$$

It should be emphasized that the present investigation of the supersonic calibration of a Stanton tube cannot be considered complete. Experiments performed in wind tunnels with more control of the uniformity of the flow and with larger ranges of parameters (variable density level would be desirable) would certainly throw more light on the problem.

IX. EXPERIMENTAL RESULTS

The undisturbed boundary layer used in the present investigation has the following characteristics at the point of measurement:

Reynolds number based on momentum thickness	$R_\theta \doteq 2500$
Skin friction coefficient	$c_f \doteq 0.0029$
Shear stress on surface	$\tau_{w_1} \doteq 1030$ dyn. cm.$^{-2}$
Reynolds number per unit length	$R \doteq 1.2 \times 10^5$ cm.$^{-1}$
Mach number	$M_1 \doteq 1.48$

It should be noted that, in the measurements, the movement of the sensing elements was replaced by movement of the impinging shock wave. Therefore, observations at the beginning and end of the interaction region actually correspond to a boundary layer with slightly different characteristics than those given above. It is believed, however, that although the farthest upstream and downstream measurements may be slightly doubtful, the results obtained in the center of the interaction region do not show appreciable errors due to this effect.

1. Interaction with Oblique Shock Waves

Two wedges with 2.5° and 4.6° half-angles were used to generate oblique shock waves interacting with the boundary layer. Figs. 21 and 22 show the corresponding schlieren photographs of the flow configuration.

In both cases, the qualitative behavior was the same as far as all observed quantities were concerned. Pressure distributions on the

flat plate in the interaction region are presented in Fig. 28, velocity profiles in Figs. 25 and 26, and the measured distribution of skin friction in Fig. 29. In all figures, the horizontal coordinate is the Reynolds number, R_ξ, based on the distance along the flat plate from the point where the undisturbed shock wave, extended, meets the surface. Location of this point was found from photographs.

The velocity profiles (Figs. 25 and 26) show a characteristic wavy shape ahead of the interaction point; it seems that the turbulent region outside the laminar sublayer decelerates more easily than the fluid closer to the surface. The higher the pressure increase through the shock wave, the smaller is the velocity reached in the turbulent region before re-acceleration takes place. It is possible that some errors result from the assumptions of constant static pressure and constant total energy across the boundary layer which were used in the computations of the velocity profiles from total-head measurements; it is believed, however, that the wavy shape is real and is connected with the different mechanisms responsible for transport of momentum within the laminar sublayer and in the outer, turbulent, part of the boundary layer.

The distribution of skin friction shows a rapid decrease at approximately the same point where the first pressure increase is observed. This decrease is followed by an approximately constant region of the order of four or five undisturbed boundary layer thicknesses. Finally, the shear stress increases again and seems to come close to the original values at the end of the range of observation. Fig. 29 shows the shear stress on the surface; as far as the skin friction

coefficient is concerned the behavior is almost the same because of the rather small changes in dynamic pressure through the interaction.

No separation of the boundary layer was observed in the oblique shock interactions. The maximum pressure increase ratio was 1.43 in the case of the 4.6° semi-angle wedge. Fage and Sargent observed separation in their experiments in the same Mach number range at pressure ratios above 2, while Bardsley and Mair at $M = 1.97$ believed, based on visual observation, that there was separation at a pressure ratio of about 1.5.

It should be noted here that the results are in overall qualitative agreement with the work of Fage and Sargent. One distinguishing feature is the somewhat more acute nature of the changes in shear stress observed in the present experiments. This is probably due to the small size of the tube used here. It is evident from the shape of the velocity distributions that including a large part of the turbulent region outside the laminar sublayer would necessarily lead to a "smoothing" effect. This is, in fact, demonstrated in some measurements, obtained at different tube heights, presented in Fage and Sargent's report.

2. Interaction with Normal Shock

A normal shock was produced in the wind tunnel by adjusting the 4.6° semi-angle wedge to such a high angle of attack that the flow between the wedge and the flat plate became choked (Fig. 23). Although this configuration did not lead to uniform flow conditions behind the shock, it was nevertheless decided worthy of investigation in order to observe the behavior of the Stanton tube in the presence of a strong

pressure gradient. The same flow parameters were observed as in the oblique shock interactions and the results are presented in Figs. 27 to 29. The origin of the streamwise coordinate is based on the bifurcation point of the shock wave. The distance from this point was observed photographically.

A separated region was apparent in the distributions of all observed quantities, especially clearly in the skin friction (Fig. 29). It should be noted that the separation started when only a part of the theoretical pressure rise had been reached, and the boundary layer reattached while the pressure was still strongly increasing. In Fig. 28, the reattachment corresponds, approximately, to the end of the flat part in the pressure distribution. The total length of the separation "bubble" was about eight undisturbed boundary layer thicknesses, and the height one-half, as can be seen from the velocity profiles in Fig. 27. The velocity profiles now showed the wavy shape with the velocity in the turbulent region decelerating all the way to zero. It is believed that in the case of the normal shock, use of the constant static pressure and constant total energy assumptions causes considerable errors in the velocity distributions. Another source of error is a slight fluctuation observed in the flow configuration.

The flow downstream of the lambda-like root of the shock wave and the following weak expansion fan was observed to be still supersonic outside the boundary layer, with a smooth compression to lower velocities. At the last point of measurement, the flow outside the boundary layer had reached nearly sonic velocity. It is believed, however, that the large extent of supersonic flow was, in this case, induced

by the acceleration of the upper subsonic flow about the wedge.

Fig. 23 does not reveal much detail of the separation phenomenon. By visual observation of the schlieren picture, one would be inclined to expect the separated region to extend far downstream; in fact, as is shown by the skin friction measurements, it ended at about the downstream edge of the lambda-like compression region.

Fig. 24 shows an interaction observed downstream of the expansion fan from the wedge shoulder in the 4.6° semi-angle case. A normal shock occurred here at a Mach number of about 1.8, and some details of the separation are clearly visible. No measurements could be obtained with this configuration.

X. CONCLUSIONS

The Stanton tube, calibrated with the floating element skin friction meter, is shown to be a useful instrument for measurement of skin friction in the presence of strong pressure gradients in compressible flow.

In supersonic flow, a marked, Mach number dependent, increase of the Stanton tube pressure was observed. Further experimental work, with larger variations of parameters than was possible in the present case, is needed in order to establish more accurately the nature and magnitude of this effect.

Distributions of surface shear stress were obtained in a turbulent boundary layer at $M = 1.48$, in the interaction region with oblique and normal shock waves. The measurements showed the expected decrease of the skin friction, followed by an increase close to the original value; with the normal shock, a closed separated region was observed.

APPENDIX

CALIBRATION OF A STANTON TUBE

Consider first incompressible flow. The difference $p_t - p$ between the Stanton tube pressure and the static pressure is assumed to depend upon τ_w, μ, ρ, h, that is, upon shearing stress on the surface, the viscosity and density of the fluid, and the height of the Stanton tube. Dimensional analysis leads to

$$\Delta p \equiv p_t - p = \tau_w \cdot Fn \left(\frac{\tau_w \rho h^2}{\mu^2} \right) \qquad (1)$$

Call u_h the value at $y = h$. For small values of $\rho u_h h/\mu$ one deals with Stokes flow and thus pressure differences should be proportional to μ. Since $\tau_w \sim \mu (u_h/h)$ it follows from Eq. (1) that

$$Fn = \text{CONST.} \qquad \text{for} \quad \frac{\rho u_h h}{\mu} \ll 1 \qquad \text{(Stokes Flow)} \qquad (2)$$

If $\rho u_h h/\mu \gg 1$ the Stanton tube behaves like an ordinary total-head tube, averaging the total pressure at its opening. In this case the pressure difference can be expected to be proportional to ρu_h^2. It follows from Eq. (1)

$$Fn \sim \frac{\tau_w \rho h^2}{\mu^2} \qquad \text{for} \quad \frac{\rho u_h h}{\mu} \gg 1 \qquad (3)$$

Thus the pressure increase read by a Stanton tube is related to the shearing stress τ_w in these limiting cases by:

$$\Delta p = \text{CONST.}\ \tau_w \qquad \frac{\rho u_h h}{\mu} \ll 1 \qquad (2a)$$

$$\Delta p = \text{CONST.}\ \tau_w^2\ \frac{\rho h^2}{\mu^2} \qquad \frac{\rho u_h h}{\mu} \gg 1 \qquad (3a)$$

Multiplying both sides of Eq. (1) by $\rho h^2/\mu^2$ we obtain

$$\frac{\Delta p\, \rho h^2}{\mu^2} = \frac{\tau_w \rho h^2}{\mu^2} \; Fn \left(\frac{\tau_w \rho h^2}{\mu^2} \right) \tag{1a}$$

which can also be written

$$\frac{\Delta p\, \rho h^2}{\mu^2} = fn \left(\frac{\tau_w \rho h^2}{\mu^2} \right) \tag{1b}$$

In terms of the general calibration parameters the limiting cases become

$$\frac{\Delta p\, \rho h^2}{\mu^2} = \text{CONST.} \; \frac{\tau_w \rho h^2}{\mu^2} \qquad \frac{\rho u_h h}{\mu} << 1 \tag{2b}$$

$$\frac{\Delta p\, \rho h^2}{\mu^2} = \text{CONST.} \left(\frac{\tau_w \rho h^2}{\mu^2} \right)^2 \qquad \frac{\rho u_h h}{\mu} >> 1 \tag{3b}$$

Taylor (Ref. 34), who first suggested Eq. (2a), found experimentally the value of the constant equal to 1.2. The constant appearing in the other limiting case (Eqs. (3a) and (3b)) has not been determined.

At high speeds two effects will be felt: First, the temperature variation in the boundary layer will cause the parameters ρ and μ to vary across the layer, and second, the displacement effect due to the tube may become important. If one calculates the variation of temperature across the opening of the Stanton tube, it can be easily seen that the first effect is not sufficient to account for the observed change of calibration with Mach number at supersonic speeds. On the other hand, even relatively small deflection angles of the flow could produce pressure rises of the observed magnitude through shock waves in the supersonic part of the boundary layer.

REFERENCES

1. Dhawan, S.: Direct Measurements of Skin Friction. Ph.D. Thesis, California Institute of Technology (1951). Also, NACA TN 2567 (1952).

2. Kempf, G.: Neue Ergebnisse der Widerstandsforschung. Werft, Reederei, Hafen, Vol. 10, pp. 234 and 247, (1929).

3. Schultz-Grunow, F.: Neues Widerstandsgesetz für glatte Platten. Luftfahrtforschung, Vol. 17, p. 239, (1940). Also, NACA TM 986, (1941).

4. Coles, D.: Direct Measurement of Supersonic Skin Friction. Reader's Forum, Journal of the Aeronautical Sciences, Vol. 19, No. 10, p. 717, (1952).

5. Bradfield, W. S., DeCoursin, D. G., and Blumer, C. B.: Characteristics of Laminar and Turbulent Boundary Layer at Supersonic Velocity. University of Minnesota, Institute of Technology, Department of Aeronautical Engineering, Rosemount Research Laboratories, Research Report 83, (1952).

6. Wieghardt, K.: Erhöhung des turbulenten Reibungswiderstandes durch Oberflächenstörungen. Jahrbuch der Deutschen Luftfahrtforschung, (1943). Also, Forschungsbericht 1563, Zentrale für Wissenschaftliches Berichtswesen, (1942). Translation, M.A.P. Volkenrode, M.A.P. - VG 129 - ...T.

7. Tillmann, W.: Supplementary Report to the above. Report of Kaiser-Wilhelm Institut für Strömungsforschung, Göttingen (1944).

8. Hoerner, S.: Aerodynamic Drag. Sighard F. Hoerner, 148 Busteed, Midland Park, New Jersey, (1951).

9. Coles, D.: Measurements in the Boundary Layer on a Smooth Flat Plate in Supersonic Flow. Ph.D. Thesis, California Institute of Technology (1953).

10. von Kármán, Th.: Mechanische Ähnlichkeit und Turbulenz. Verhandlungen der III Internationalen Kongress für Technische Mechanik, Stockholm, p. 85, (1931).

11. von Kármán, Th.: Turbulence and Skin Friction. Journal of the Aeronautical Sciences, Vol. 1, No. 1, (1934).

12. Wilson, R. E.: Turbulent Boundary Layer Characteristics at Supersonic Speeds - Theory and Experiment. University of Texas. Defense Research Laboratory Report 221 (CM-569), (1949). Also, Journal of the Aeronautical Sciences, Vol. 17, No. 9, (1950).

13. Rubesin, M. W., Maydew, R. C., and Varga, S. A.: An Analytical and Experimental Investigation of the Skin Friction of the Turbulent Boundary Layer on a Flat Plate at Supersonic Speeds. NACA TN 2305, (1951).

14. Goldstein, S.: Modern Developments in Fluid Dynamics, Vol. II. Oxford University Press, (1938).

15. Schlichting, H.: Grenzschicht-Theorie. Verlag G. Braun, Karlsruhe, (1951).

16. von Kármán, Th.: The Problem of Resistance in Compressible Fluids. Proc. Fifth Volta Congress, (1935).

17. Frankl, F. and Voishel, V.: Turbulent Friction in the Boundary Layer of a Flat Plate in a Two-Dimensional Compressible Flow at High Speeds. Central Aero-Hydrodynamical Institute, Moscow, Report No. 321, (1937). Also, NACA TM 1053 (1943).

18. van Driest, E. R.: Turbulent Boundary Layer in Compressible Fluids. Journal of the Aeronautical Sciences, Vol. 18, No. 3, (1951).

19. Donaldson, C. duP.: On the Form of the Turbulent Skin Friction Law and Its Extension to Compressible Flows. NACA TN 2092, (1952).

20. Cope, W. F.: The Measurement of Skin Friction in a Turbulent Boundary Layer at a Mach Number of 2.5, Including the Effects of a Shock Wave. Proc. Royal Society, Ser. A, Vol. 215, No. 1120, p. 84, (1952).

21. Fage, A. and Sargent, R. F.: An Air-injection Method of Fixing Transition from Laminar to Turbulent Flow in a Boundary Layer. A.R.C. Reports and Memoranda No. 2106 (1944).

22. Bardsley, O.: The Conditions at a Sharp Leading Edge in Supersonic Flow. Phil. Mag., Ser. 7, Vol. XLII, (1951).

23. Gazley, Carl Jr.: Boundary Layer Stability and Transition in Subsonic and Supersonic Flow. Journal of the Aeronautical Sci., Vol. 20, No. 1, (1953).

24. Wilson, R. E. and Young, E. C.: Aerodynamic Interference of Pitot Tubes in a Turbulent Boundary Layer at Supersonic Speed. University of Texas, Defense Research Laboratory, Report No. DRL-228 (CF-1351), (1949).

25. Ackeret, J., Feldmann, F., and Rott, N.: Untersuchungen an Verdichtungsstössen und Grenzschichten in Schnell Bewegten Gasen. Mitteilungen aus dem Institut für Aerodynamik an der Eidgenössischen Technischen Hochschule in Zürich, No. 10, (1946). Also, NACA TM 1113, (1947).

26. Liepmann, H. W.: The Interaction Between Boundary Layers and Shock Waves in Transonic Flow. Journal of the Aeronautical Sciences, Vol. 13, No. 12, (1946).

27. Fage, A. and Sargent, R. F.: Shock Wave and Boundary Layer Phenomena Near a Flat Surface. Proc. Royal Society, Ser. A, Vol. 190, No. 1020, (1947).

28. Liepmann, H. W., Roshko, A., and Dhawan, S.: On the Reflection of Shock Waves from Boundary Layers. NACA TN 2334, (1951).

29. Barry, F., Shapiro, A. and Neumann, E.: Some Experiments on the Interaction of Shock Waves with Boundary Layers on Flat Plates. Journal of Applied Mechanics, Vol. 17, No. 2, (1950). Also, Journal of the Aeronautical Sciences, Vol. 18, No. 4, (1951).

30. Bardsley, O. and Mair, W.: The Interaction Between an Oblique Shock Wave and a Turbulent Boundary Layer. Phil. Mag., Ser. 7, Vol. 42, No. 324, (1951).

31. Bogdonoff, S. and Solarski, A.: A Preliminary Investigation of a Shockwave - Turbulent Boundary Layer Interaction. Princeton University, Aeronautical Engineering Laboratory, Report No. 184, (1951).

32. Stanton, T. E., Marshall, O., and Bryant, C. N.: On the Conditions at the Boundary of a Fluid in Turbulent Motion. Proc. Royal Society, Ser. A, Vol. 97, No. 687, (1920).

33. Fage, A. and Falkner, V. M.: An Experimental Determination of Friction on the Surface of an Airfoil. A.R.C. Reports and Momoranda No. 1315. Also, Proc. Royal Society, Ser. A, Vol. 129, No. 810, (1930).

34. Taylor, G. I.: Measurements with a Half-Pitot Tube. Proc. Royal Society, Ser. A, Vol. 166, No. 927, (1938).

TABLE I

SUBSONIC MEASUREMENTS; REYNOLDS NUMBER BASED ON DISTANCE FROM TRIP DEVICE

M	$R_x \times 10^{-6}$	$c_f \times 10^5$
0.18	0.33	417
0.20	0.36	409
0.26	0.48	395
0.27	0.48	380
0.31	0.55	384
0.33	0.59	374
0.37	0.63	366
0.46	0.76	340
0.49	0.82	344
0.56	0.90	336
0.57	0.90	337
0.65	1.00	330
0.75	1.03	301
0.85	1.12	301
0.97*	1.20	300

*At M = 0.97 a supersonic region existed near leading edge.

TABLE II

SUPERSONIC MEASUREMENTS; REYNOLDS NUMBER BASED ON DISTANCE FROM PEAK SHEAR IN TRANSITION REGION

M	$R_x \times 10^{-6}$	$c_f \times 10^5$	Average Results
1.45	1.04	300	
1.48	1.04	294	
1.49	1.04	300	
1.50	1.02	291	
1.50	1.04	302	$\underline{M = 1.50}$
1.50	1.02	302	
1.50	1.03	302	$c_f/c_{f_i} = 0.89$
1.50	1.03	292	
1.52	1.02	309	
1.52	1.02	307	
1.52	1.01	309	
1.52	1.01	307	
1.71	0.68	324	
1.72	0.67	321	$\underline{M = 1.75}$
1.73	0.66	321	
1.74	0.67	323	$c_f/c_{f_i} = 0.89$
1.75	0.67	323	
1.73	0.84	313	
1.74	0.85	319	$\underline{M = 1.75}$
1.74	0.85	319	
1.76	0.84	310	(not plotted in Fig. 16)
1.76	0.84	312	$c_f/c_{f_i} = 0.90$

Incompressible Reference: Coles

TABLE III

SUPERSONIC RESULTS; REYNOLDS NUMBER BASED ON MOMENTUM THICKNESS

M	R_θ	$c_f \times 10^5$	Average (c_f/c_{fi})
1.48	1910	315	0.92
	2340	302	
1.52	1610	324	0.91
	2030	307	
1.75	1780	323	0.93
	1920	319	

Incompressible Reference: Coles

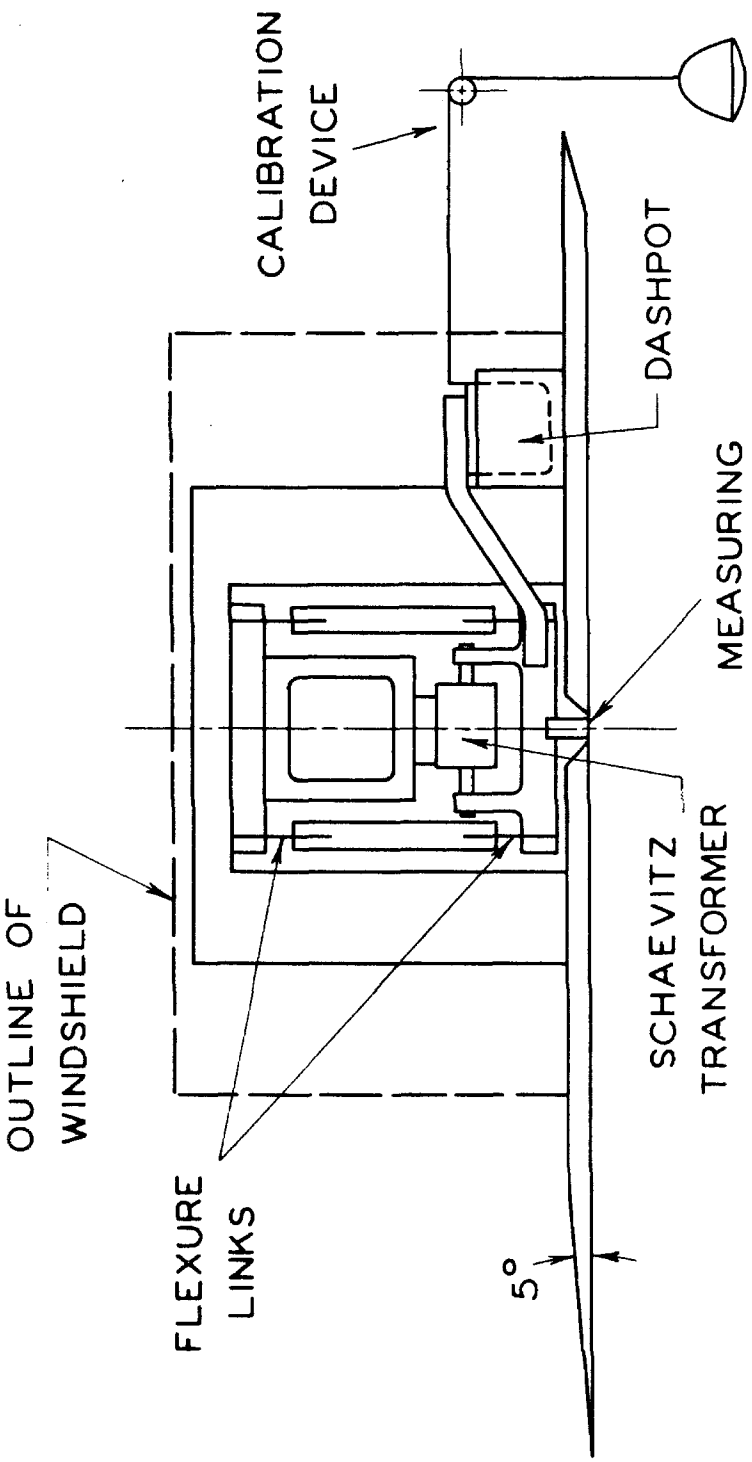

SKIN FRICTION METER

FIG. 1

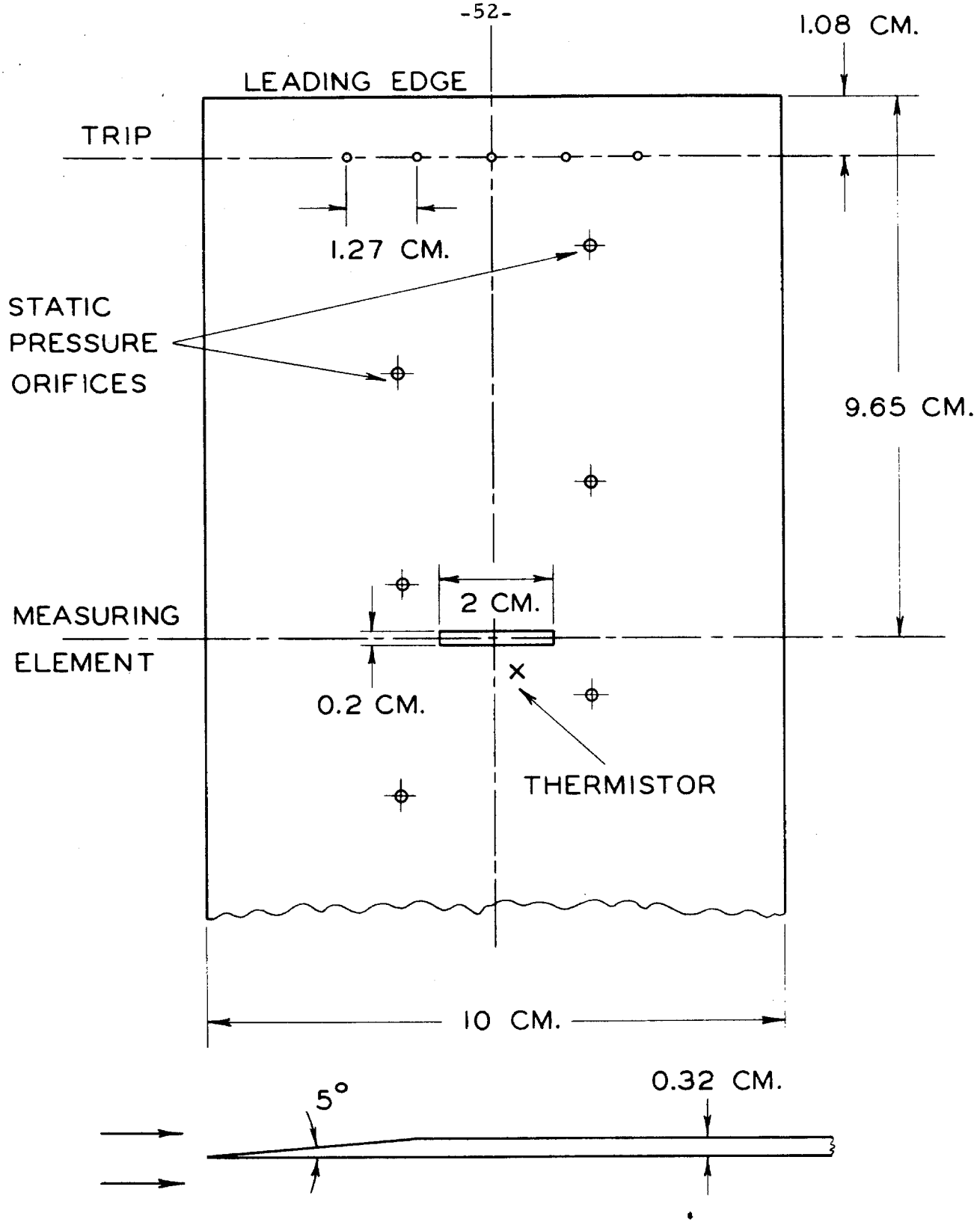

FLAT PLATE CONFIGURATION

SUPERSONIC EXPERIMENTS

FIG. 2

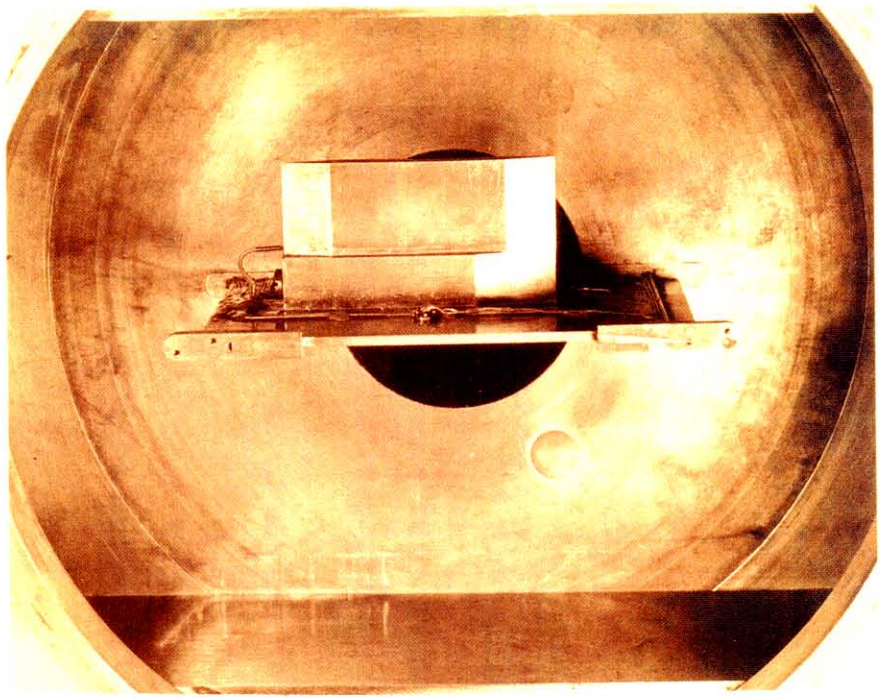

INSTALLATION OF SKIN FRICTION METER IN THE GALCIT 4" x 10" TRANSONIC WIND TUNNEL

FIG. 3

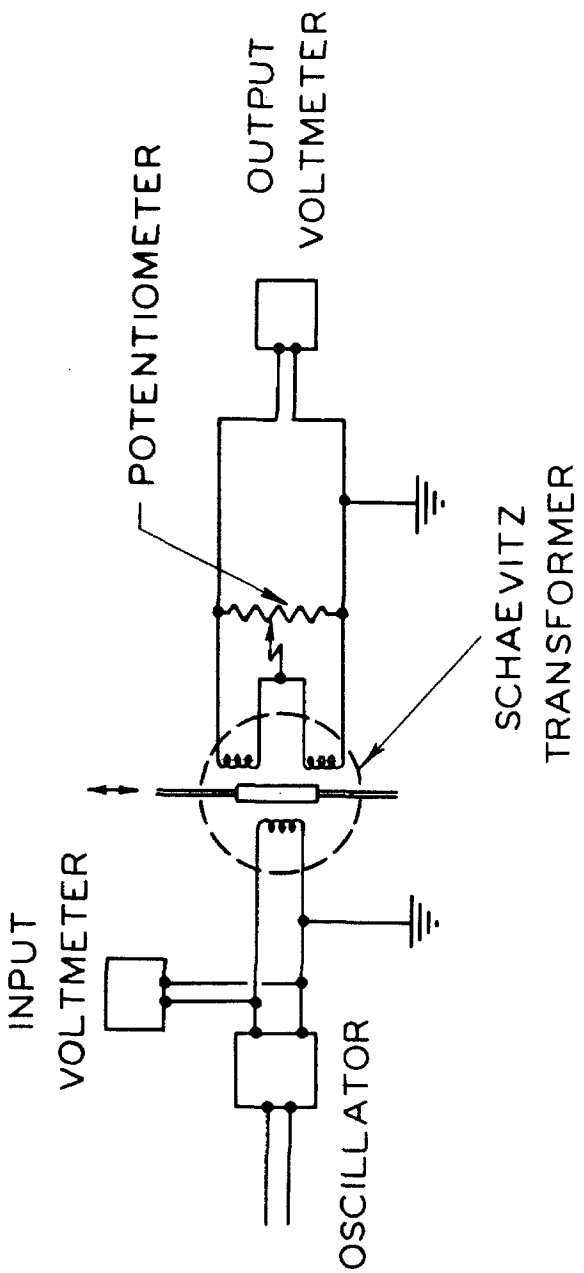

ELECTRICAL CIRCUIT

FIG. 4

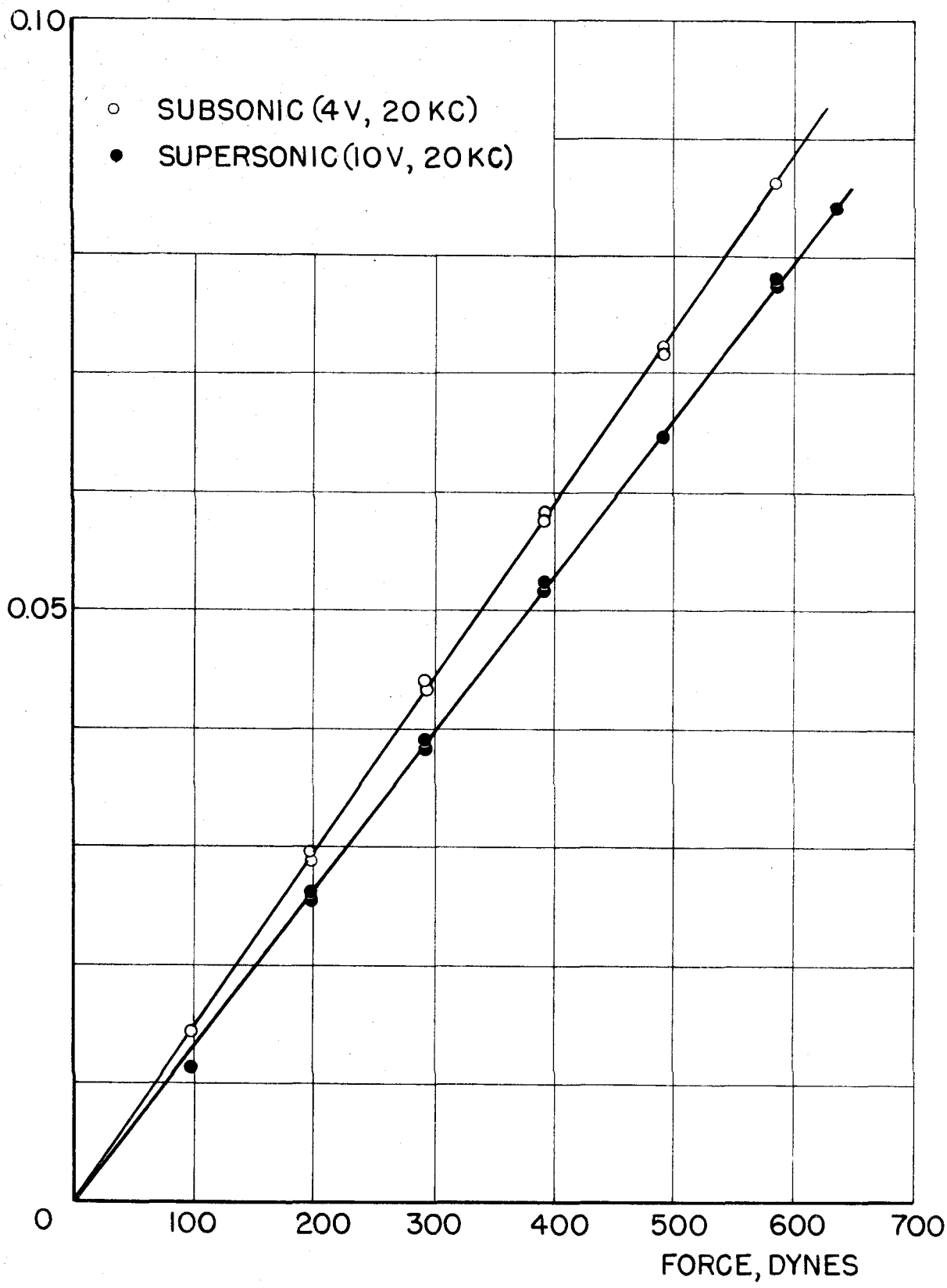

FIG. 5 - CALIBRATION OF SKIN FRICTION METER

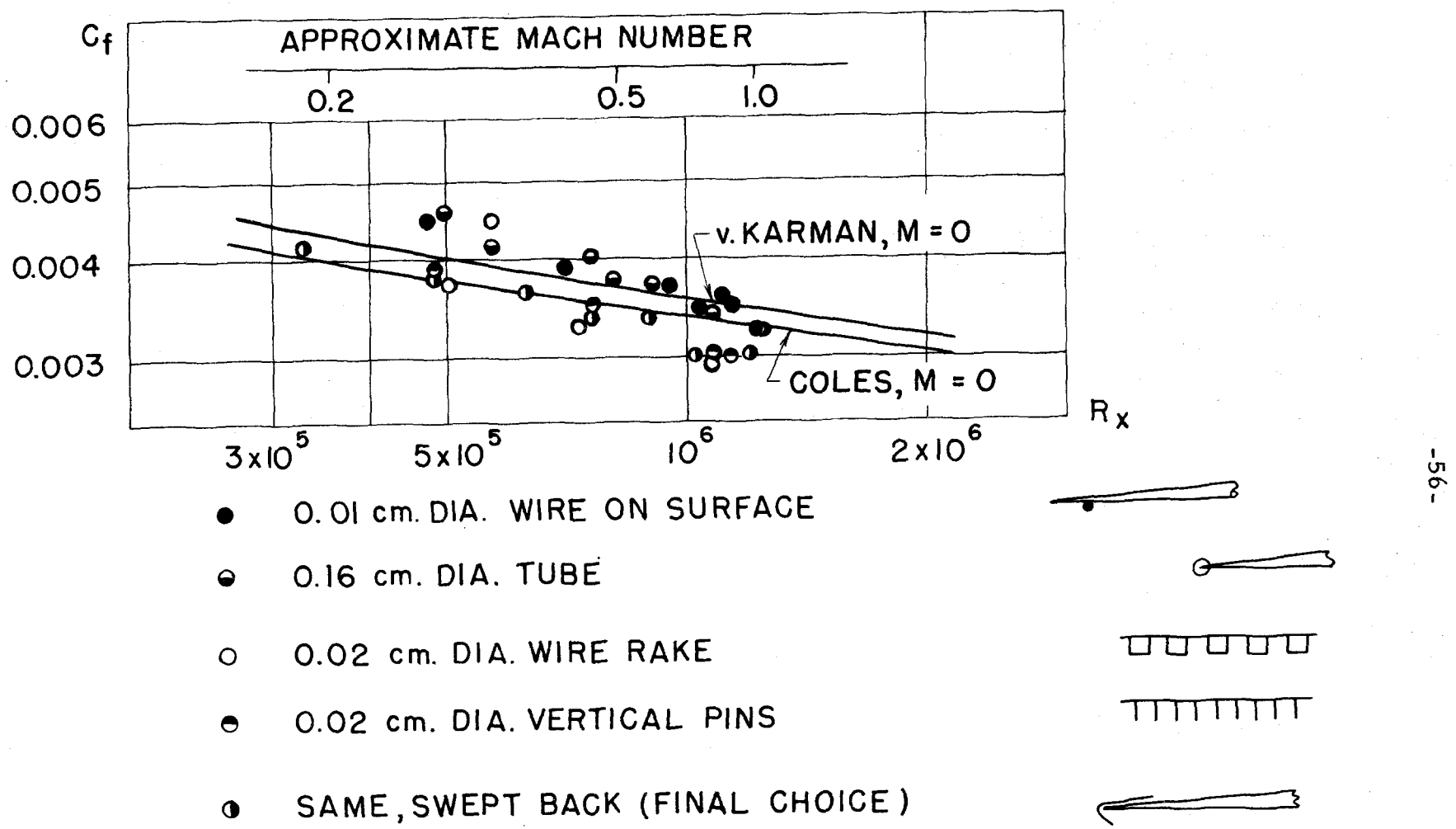

FIG.6- EFFECT OF METHOD OF TRIPPING ON LOCAL SKIN FRICTION

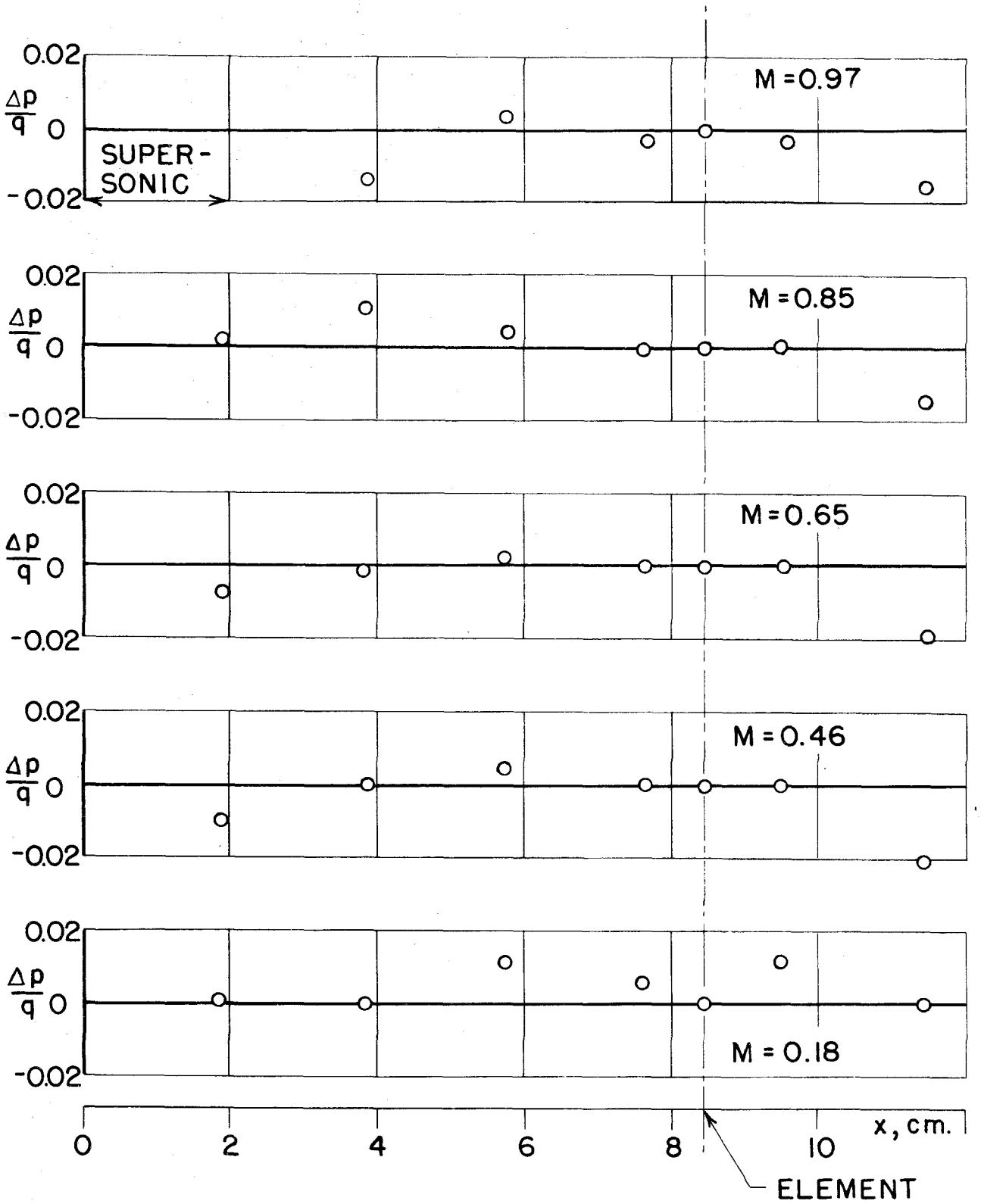

FIG. 7 - PRESSURE DISTRIBUTIONS AT SUBSONIC SPEEDS

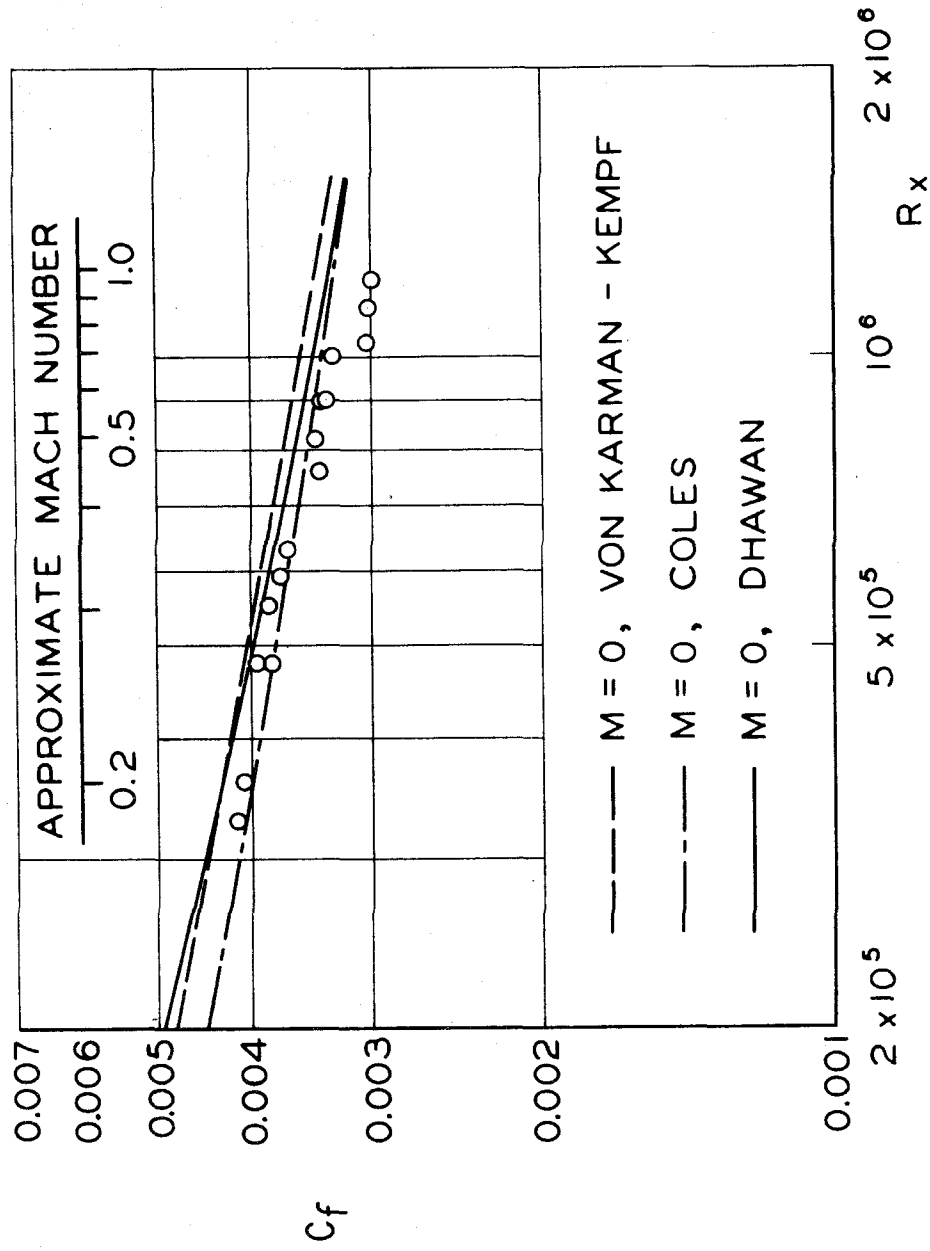

SUBSONIC MEASUREMENTS

FIG. 8

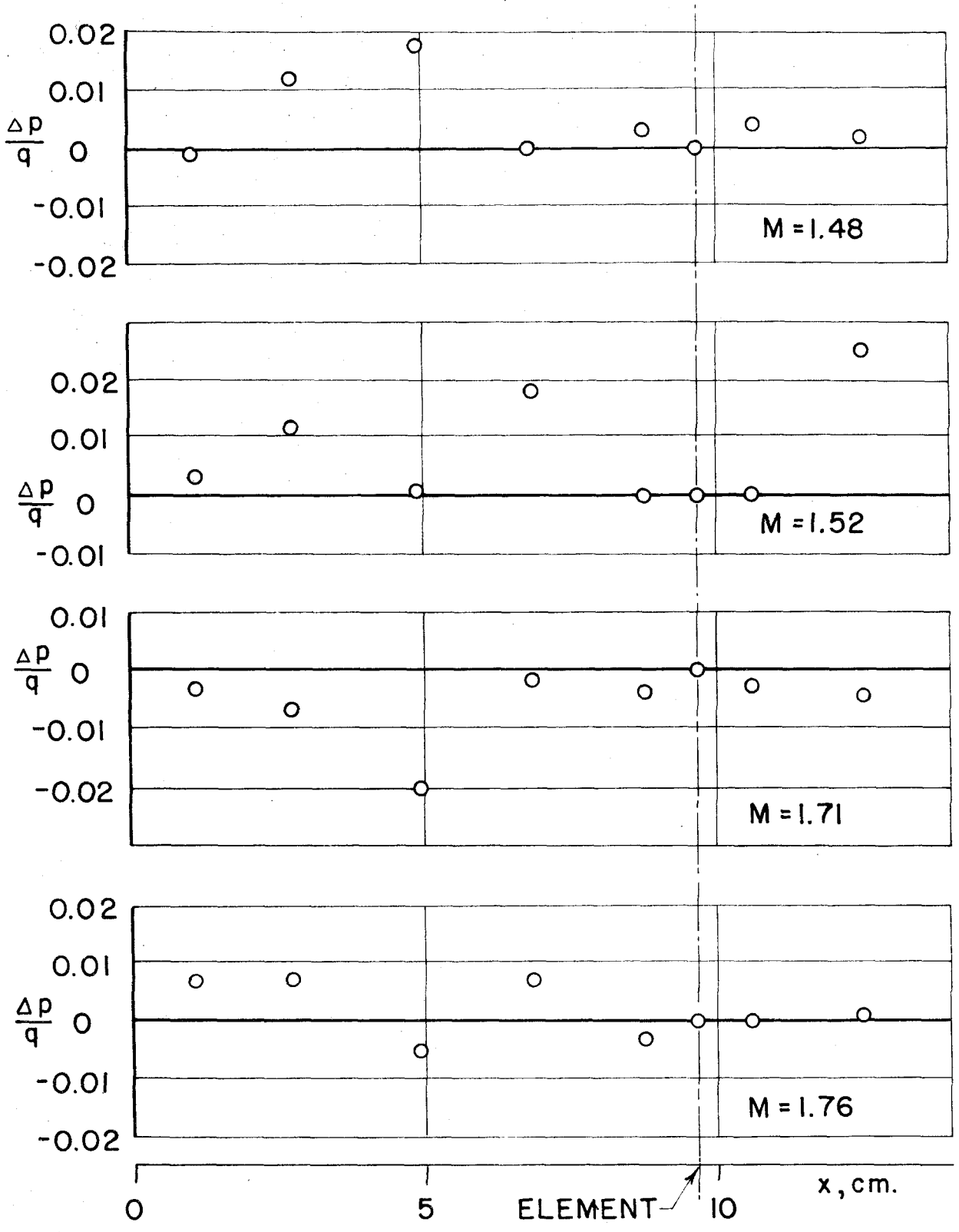

FIG. 9 – REPRESENTATIVE PRESSURE DISTRIBUTIONS AT SUPERSONIC SPEEDS

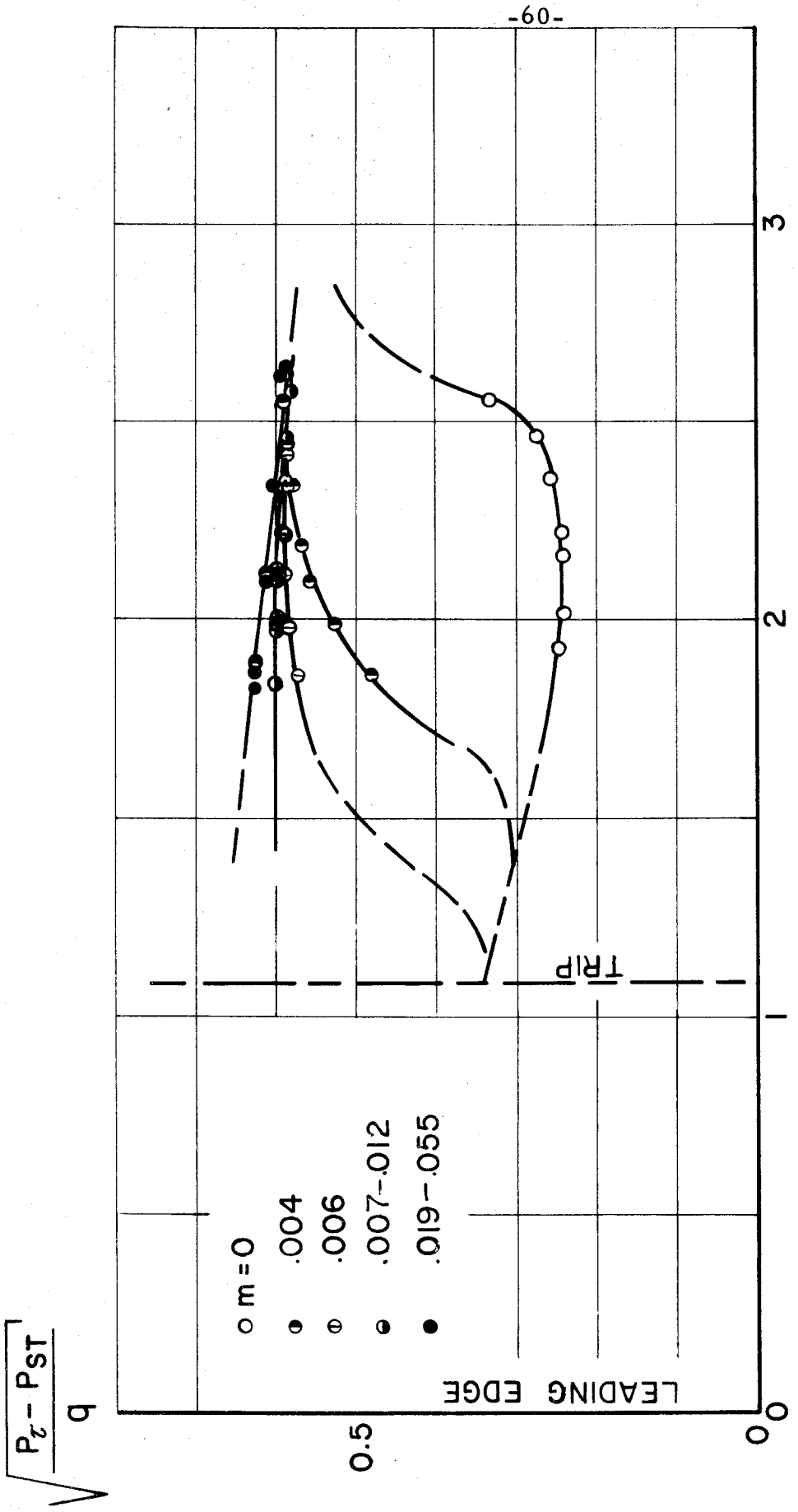

FIG. 10 - TRANSITION AT M=1.48
R=1.34 x 10^5/cm.

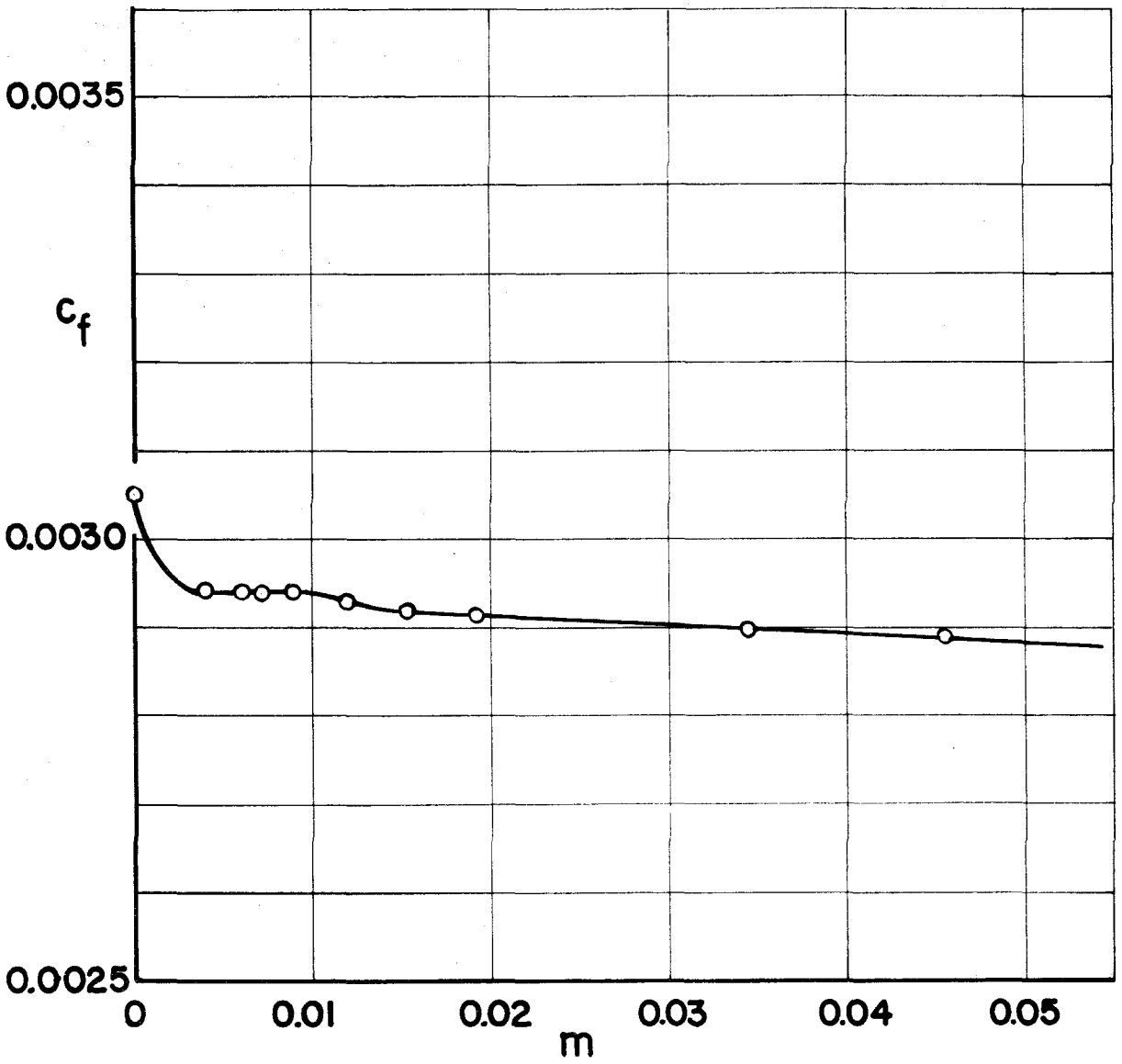

FIG. 11 – DEPENDENCE OF MEASURED SKIN FRICTION ON TRIP MASS FLOW, M = 1.48

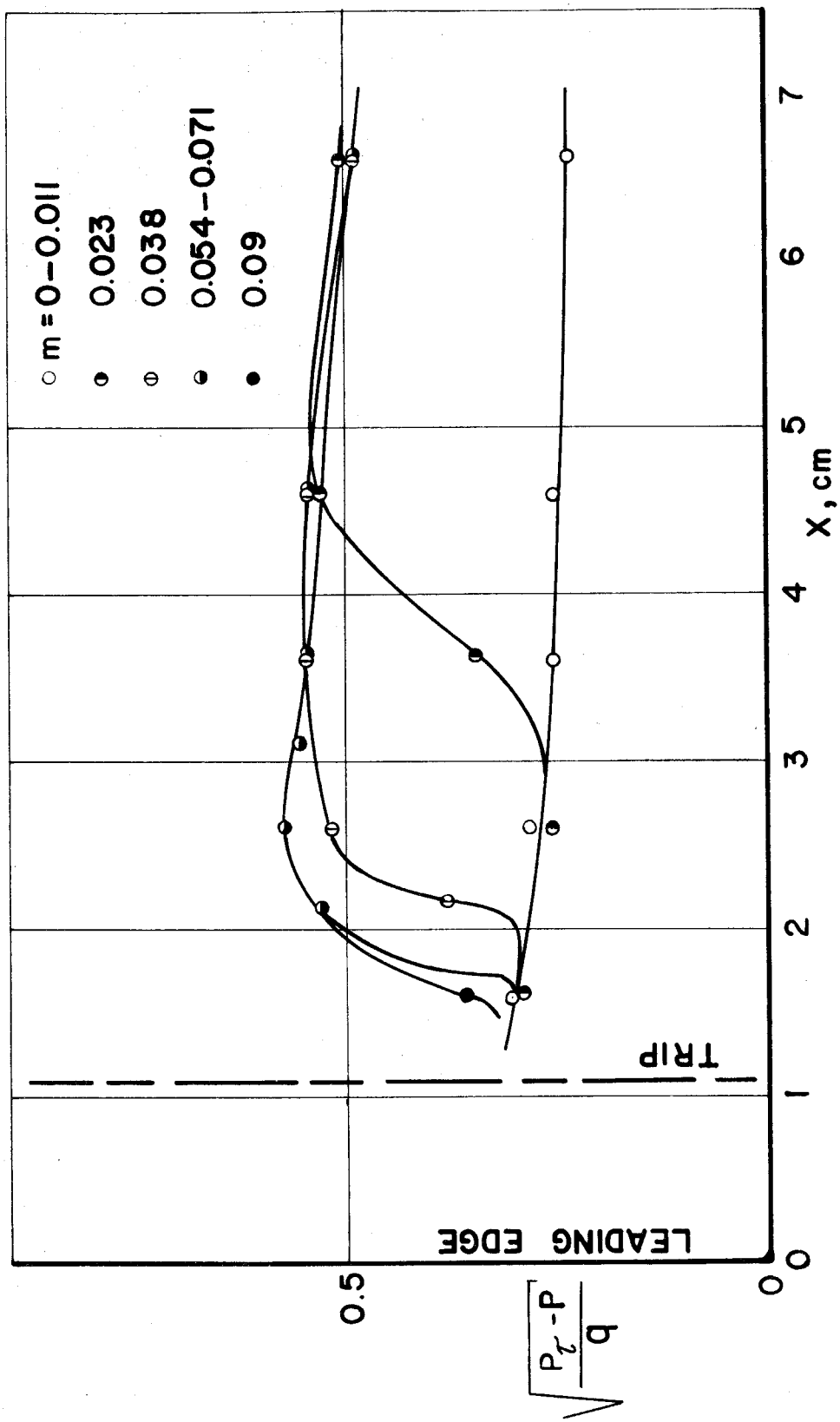

FIG.12- TRANSITION AT M=1.76

R=1.15 x 10^5/cm

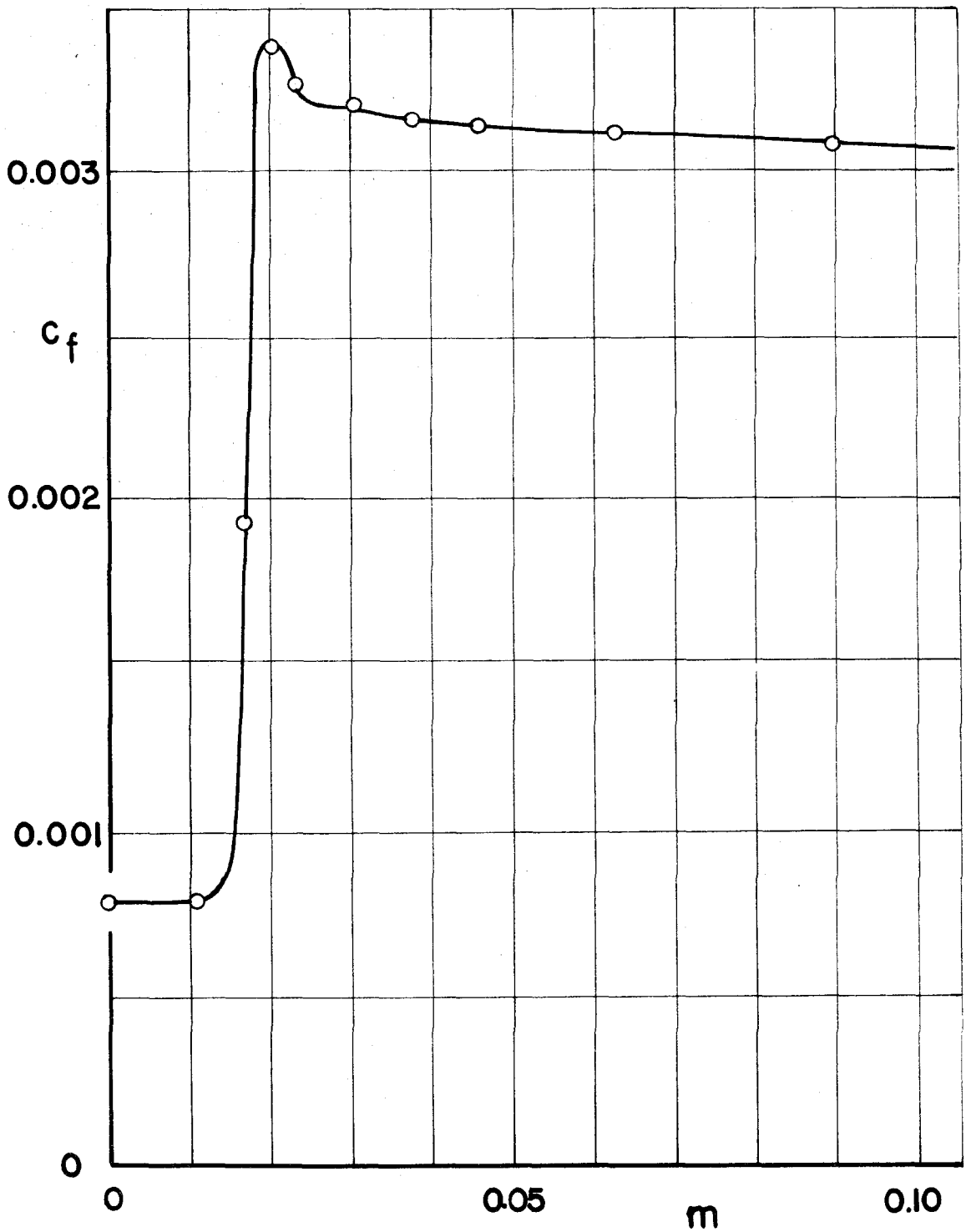

FIG. 13- DEPENDENCE OF MEASURED SKIN FRICTION ON TRIP MASS FLOW, M=1.76

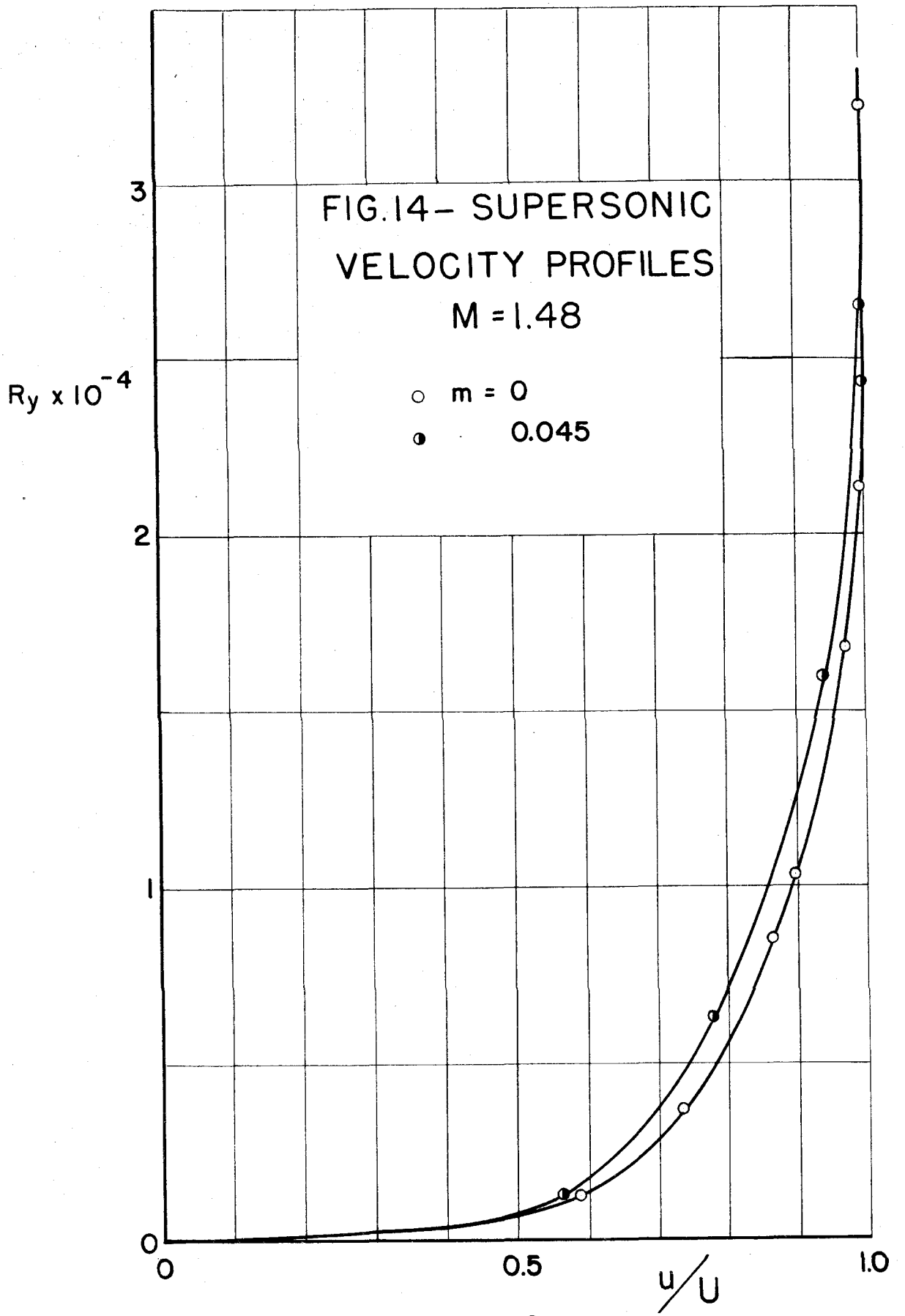
FIG.14- SUPERSONIC
VELOCITY PROFILES
M = 1.48
m = 0
0.045
$R_y \times 10^{-4}$
3
2
1
0
0
0.5
1.0
u/U

FIG.14

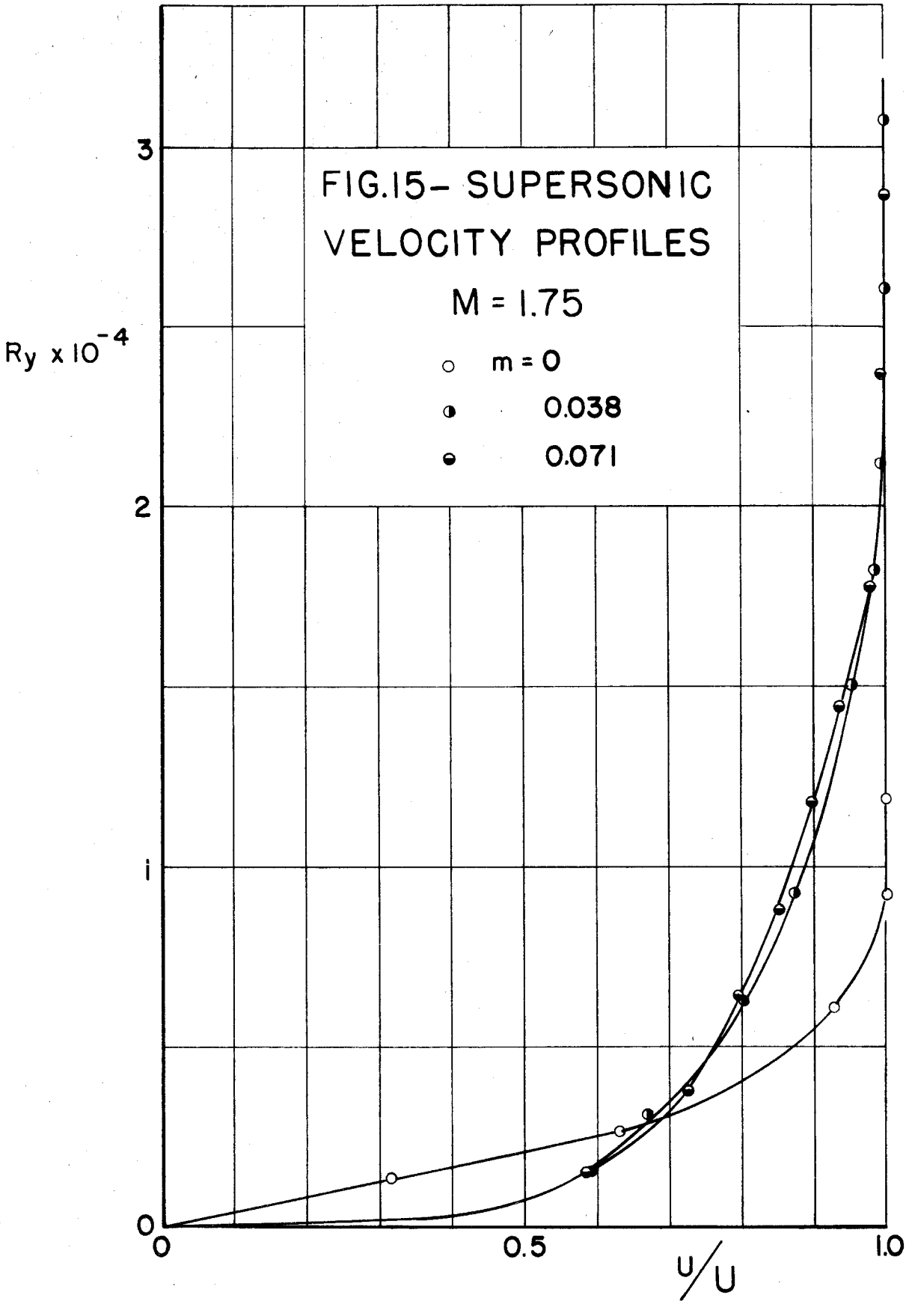
FIG.15- SUPERSONIC
VELOCITY PROFILES
M = 1.75
m = 0
0.038
0.071
Ry x 10^-4
3
2
1
0
0
0.5
1.0
U/U

FIG.15

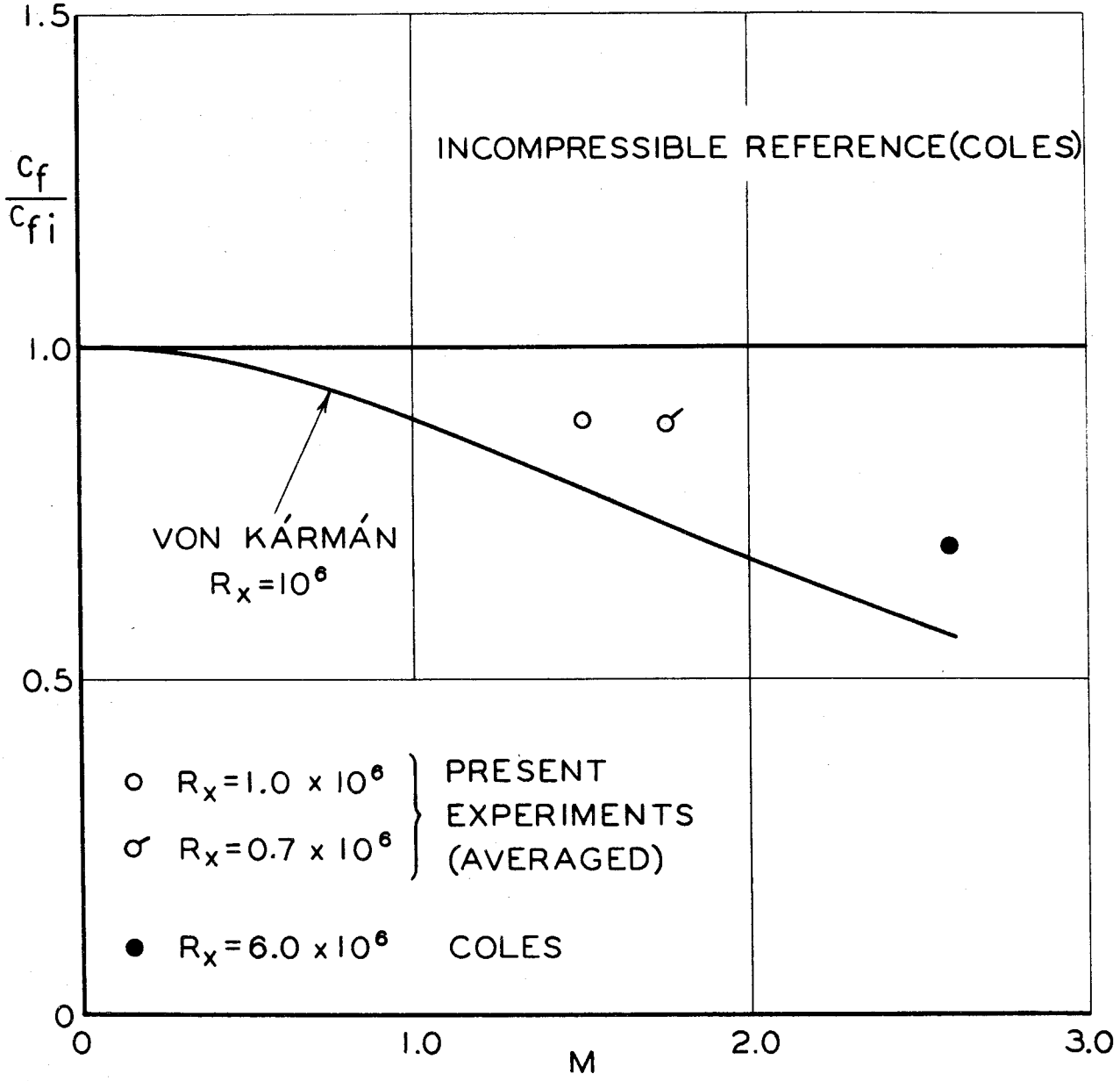

SUPERSONIC RESULTS

FIG. 16

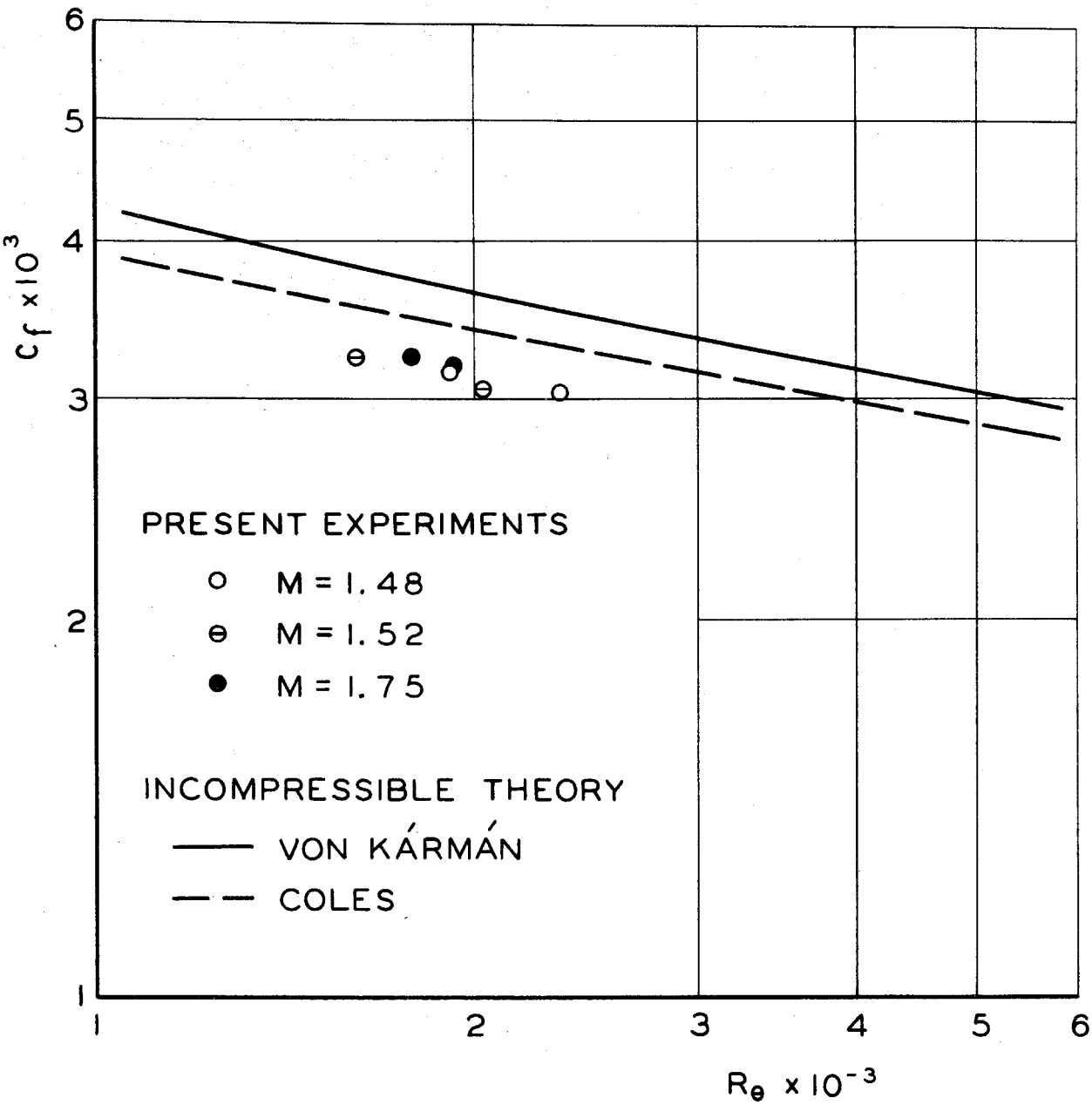

SKIN FRICTION IN TERMS OF MOMENTUM THICKNESS

FIG. 17

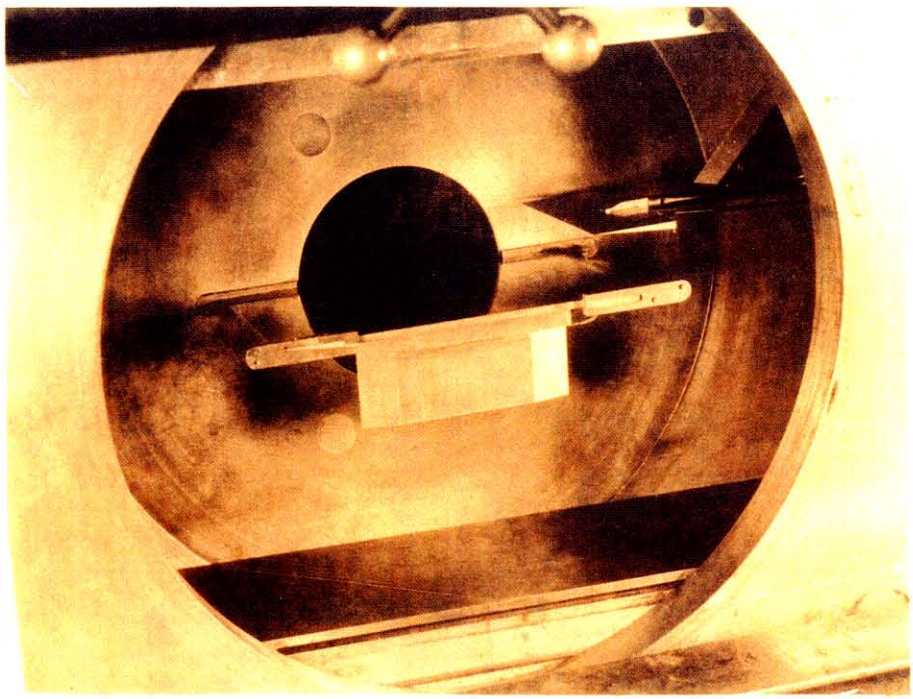

INSTALLATION OF SKIN FRICTION METER AND WEDGE

FIG. 18

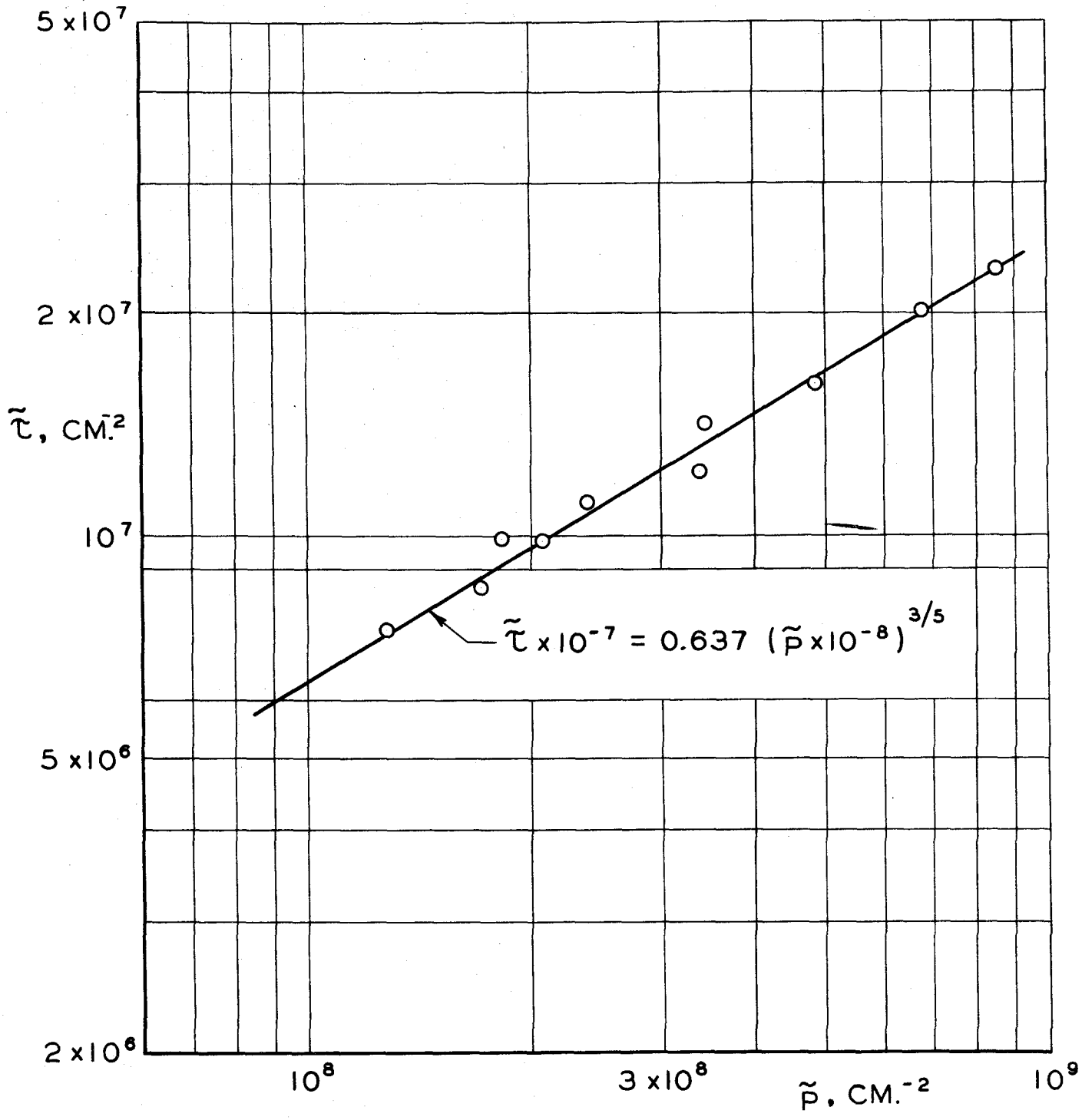

STANTON TUBE
SUBSONIC CALIBRATION

FIG. 19

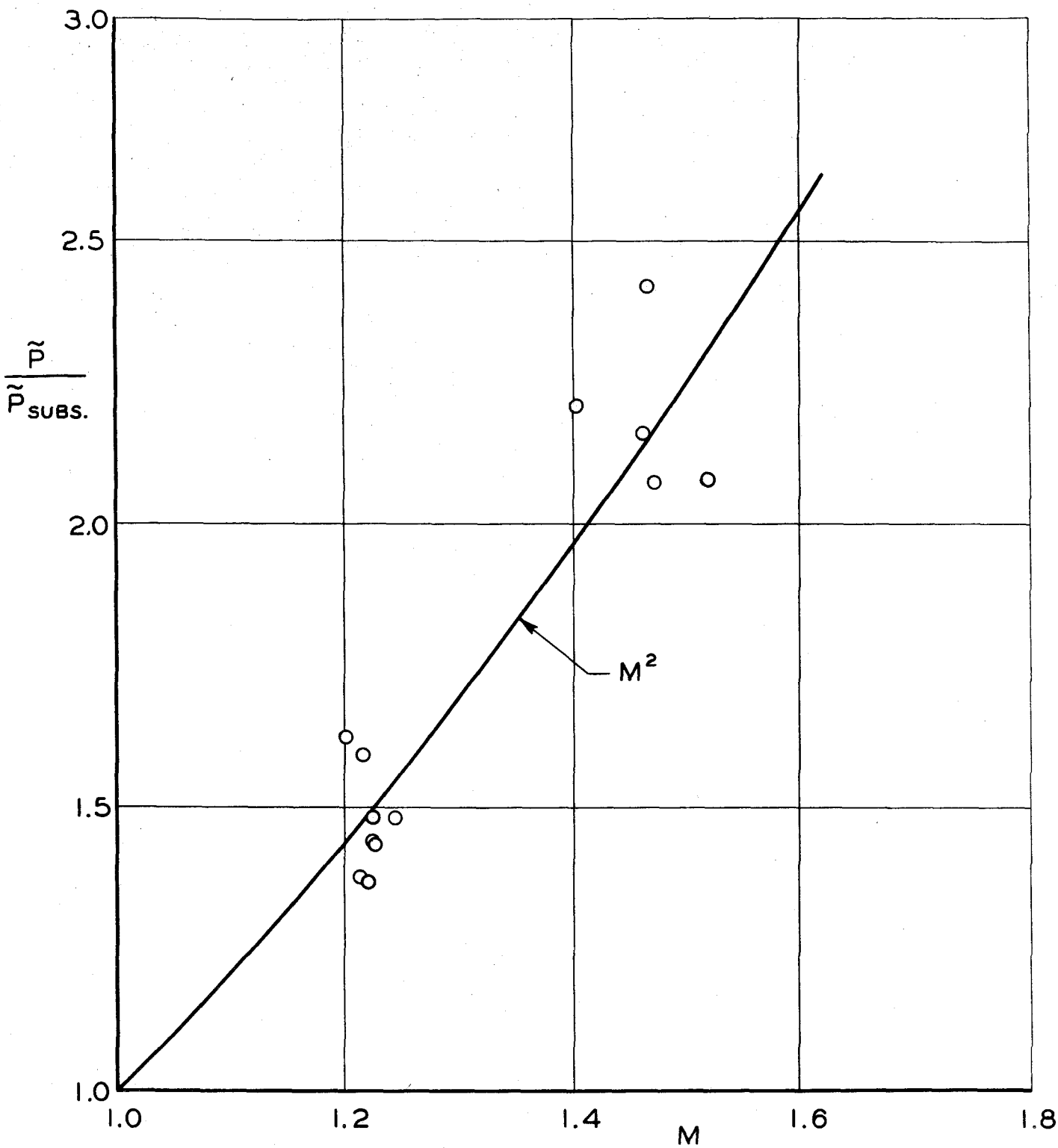

STANTON TUBE — SUPERSONIC CALIBRATION

FIG. 20

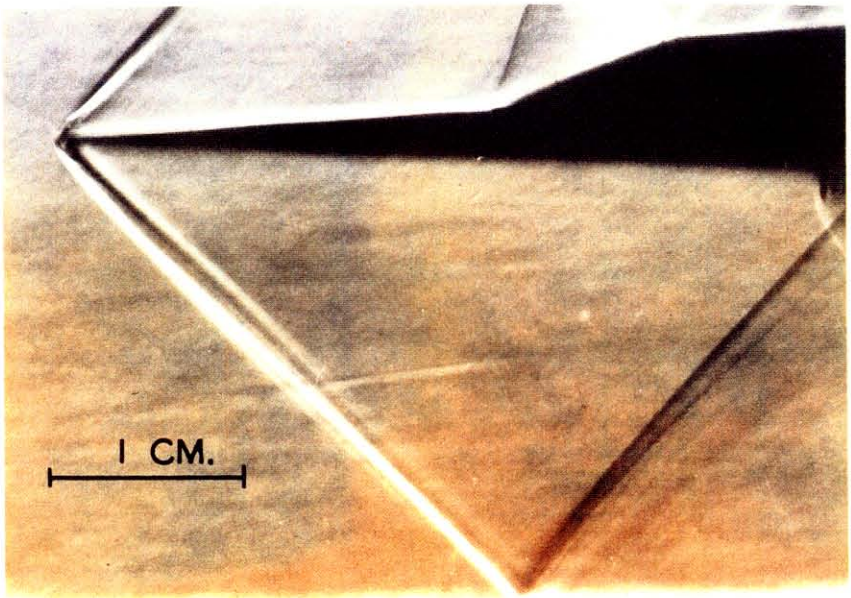

INTERACTION WITH OBLIQUE SHOCK WAVE
PRODUCED BY 2.5° HALF-ANGLE WEDGE
$M = 1.48 \quad R_{\theta} = 2500 \quad R = 1.20 \times 10^{5}$ cm.$^{-1}$

FIG. 21

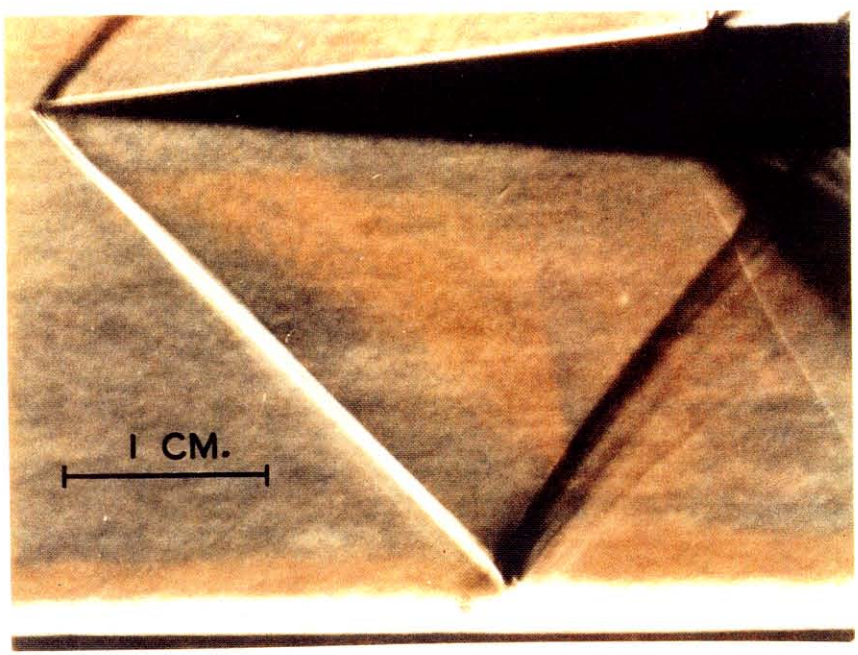

INTERACTION WITH OBLIQUE SHOCK WAVE
PRODUCED BY 4.6° HALF-ANGLE WEDGE
$M = 1.47 \quad R_{\theta} = 2500 \quad R = 1.18 \times 10^{5}$ cm.$^{-1}$

FIG. 22

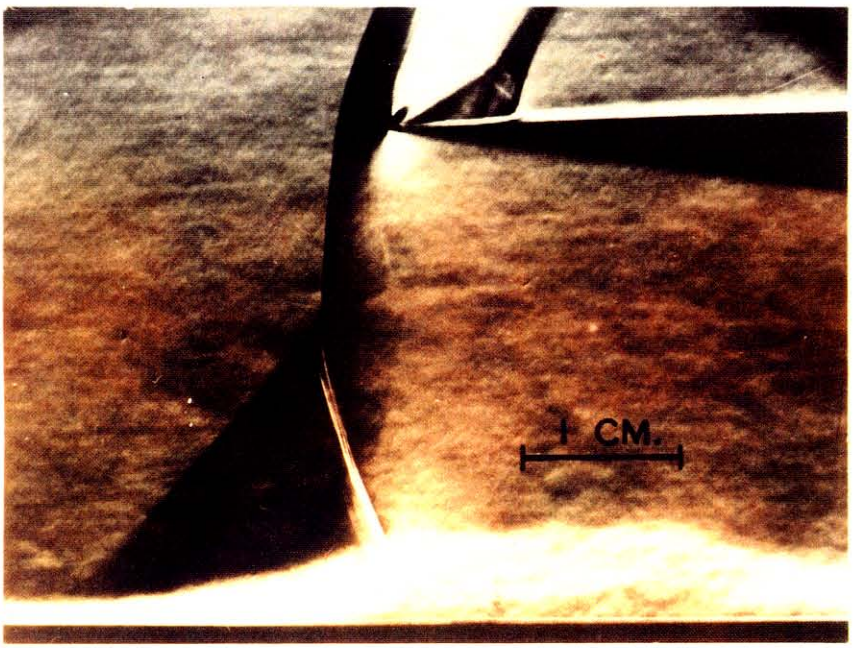

INTERACTION WITH NORMAL SHOCK

$M = 1.48 \quad R_\theta = 2500 \quad R = 1.18 \times 10^5 \text{ cm.}^{-1}$

FIG. 23

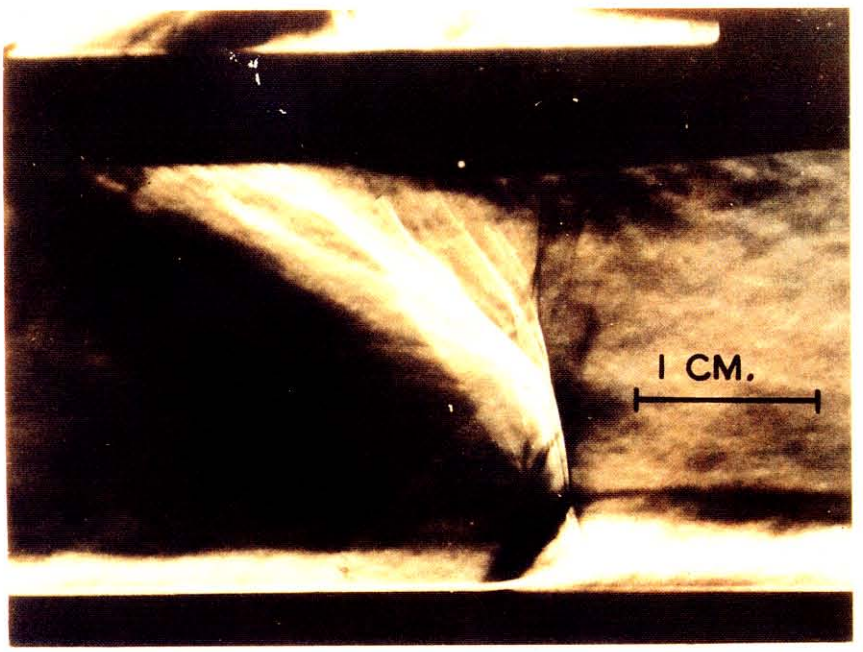

INTERACTION WITH EXPANSION FOLLOWED BY NORMAL SHOCK

FIG. 24

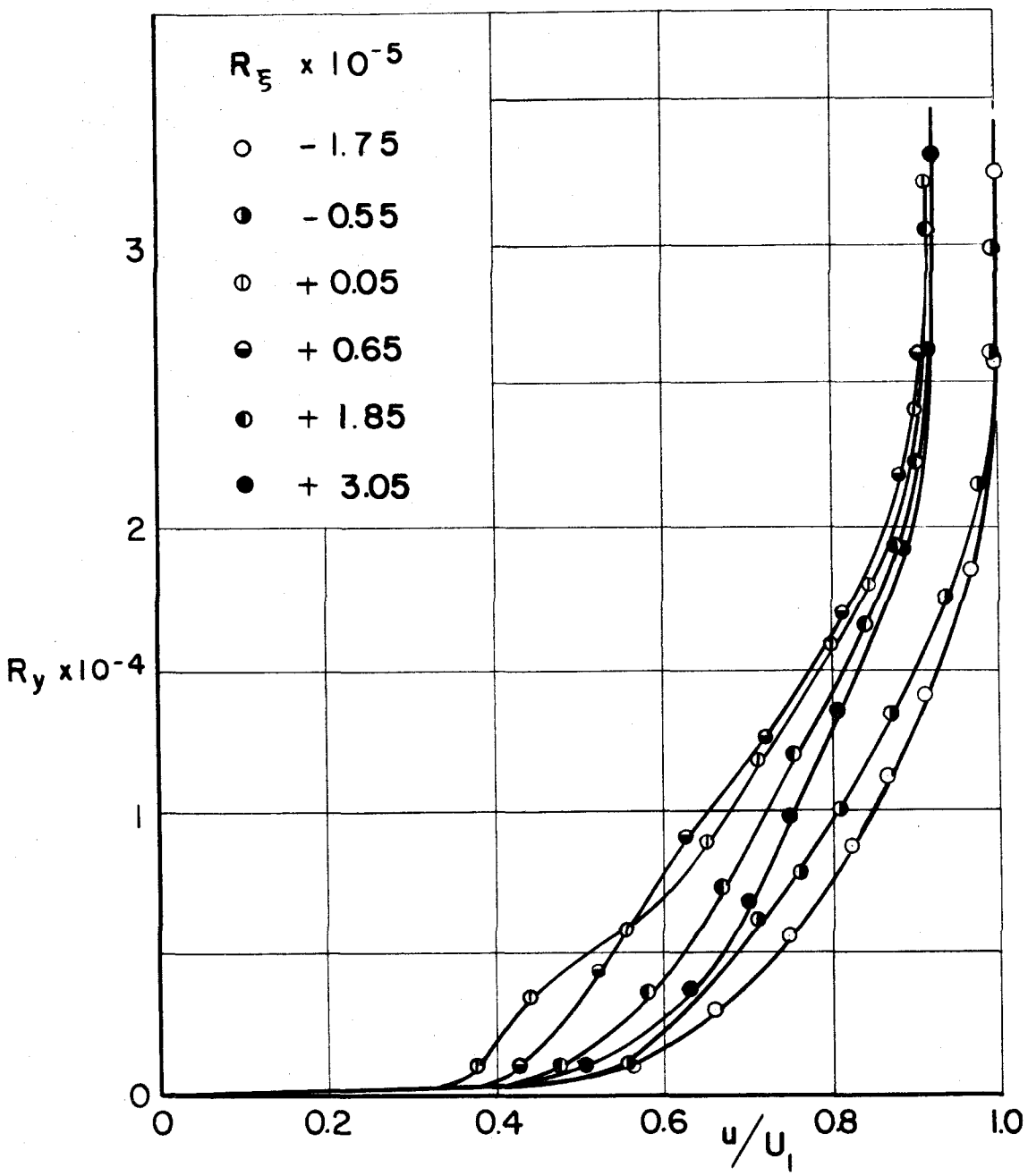

VELOCITY PROFILES

$M_1 = 1.48$, $R = 1.2 \times 10^5$ cm^{-1}

$\alpha = 2.5°$

FIG.25

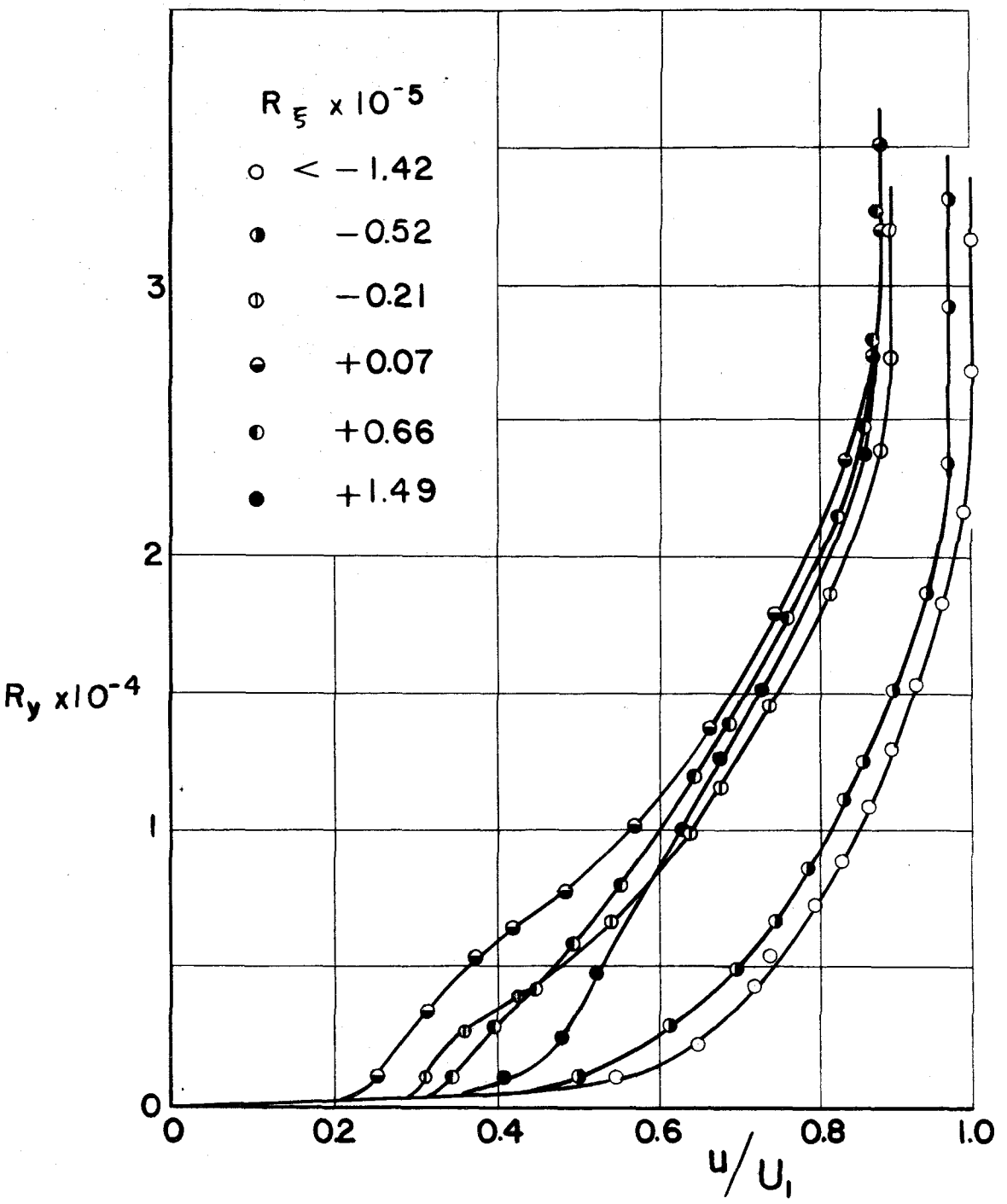

VELOCITY PROFILES

$M_1 = 1.47$, $R = 1.18 \times 10^5 cm^{-1}$

$\alpha = 4.6°$

FIG. 26

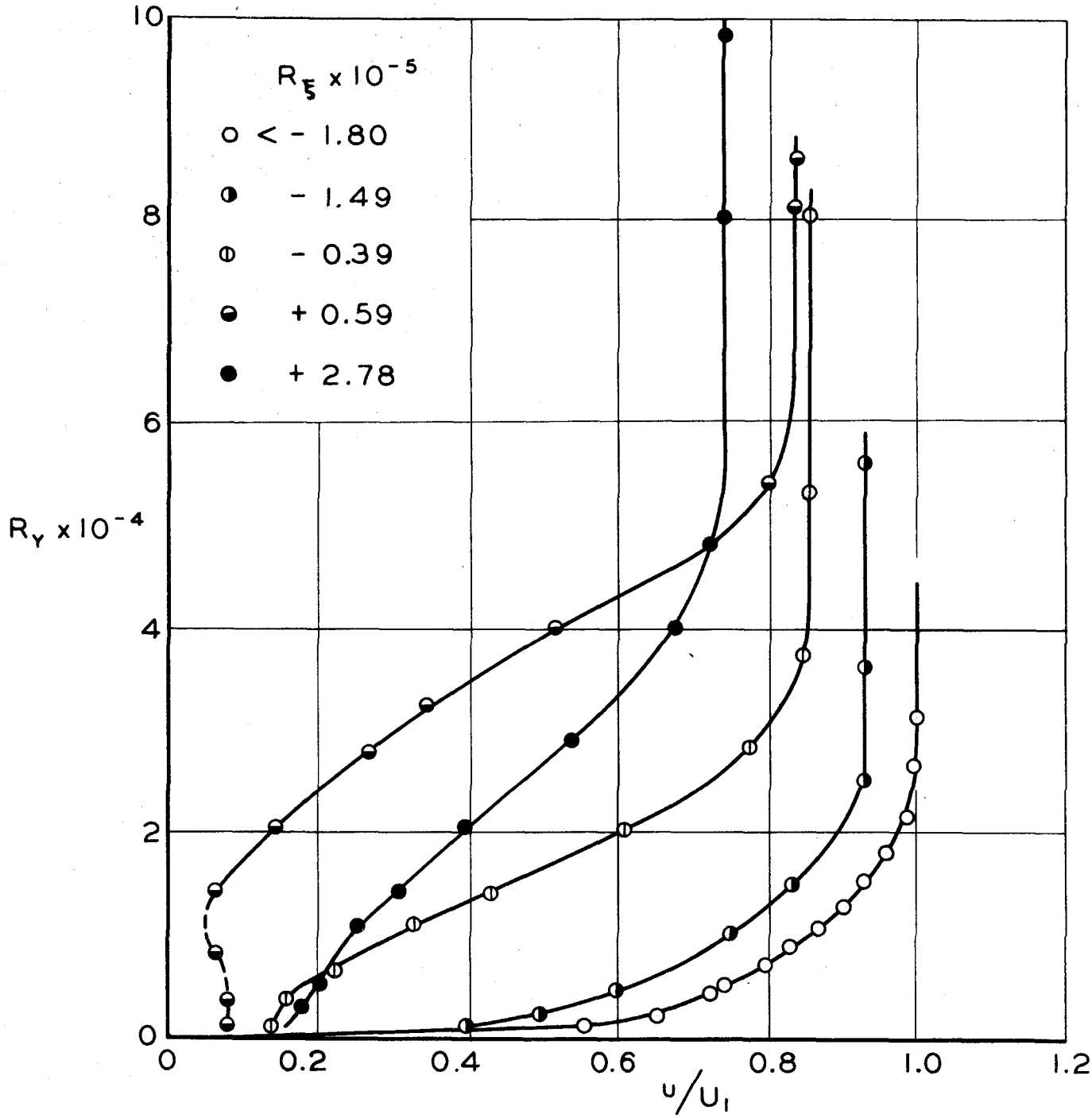

VELOCITY PROFILES

NORMAL SHOCK

$M_1 = 1.48$ $R = 1.18 \times 10^5$ CM.$^{-1}$

FIG. 27

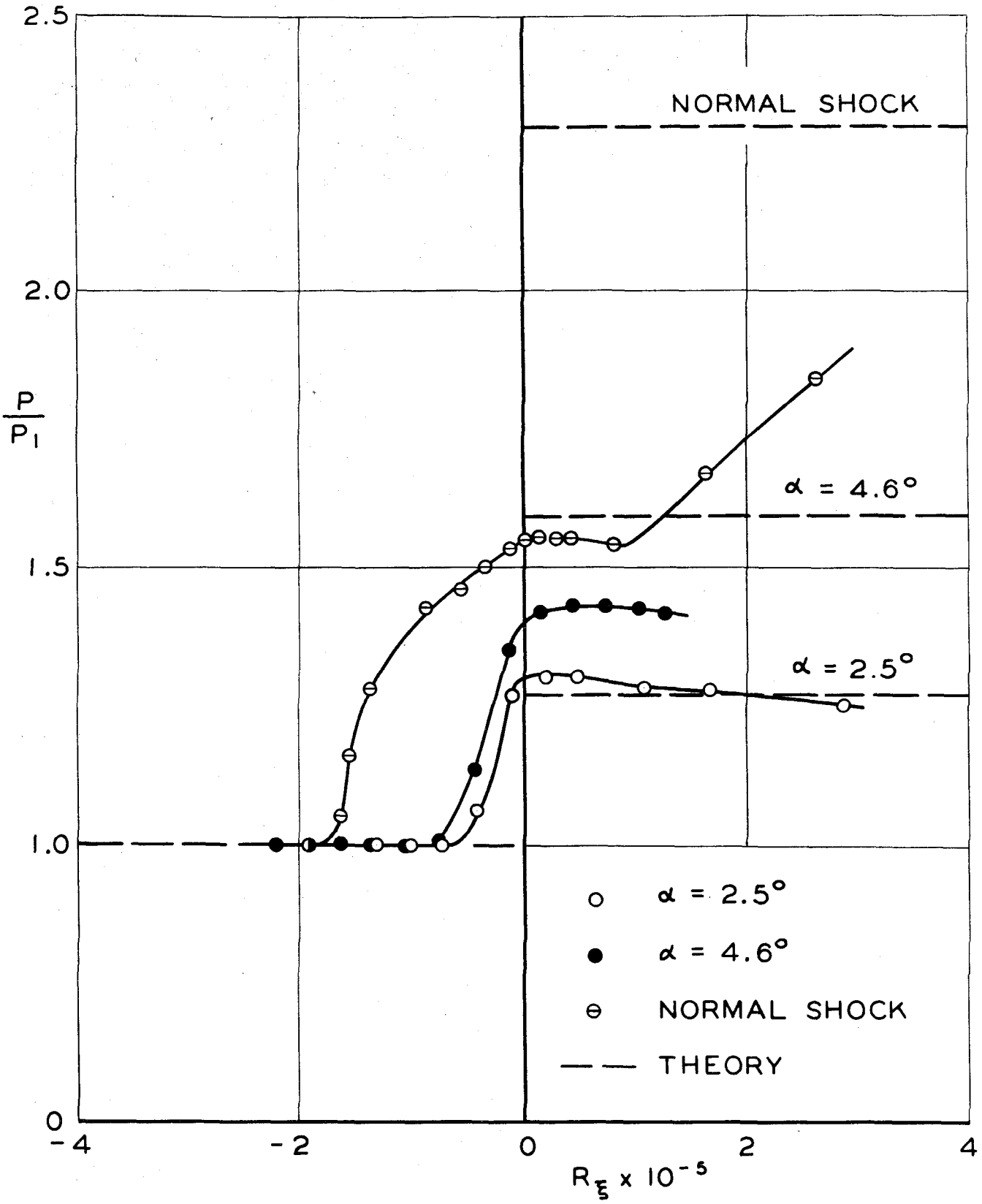

STATIC PRESSURE ON SURFACE

$M_1 \doteq 1.48$ $R \doteq 1.2 \times 10^5$ CM.$^{-1}$

$P_1 \doteq 19.3$ CM. HG

FIG. 28

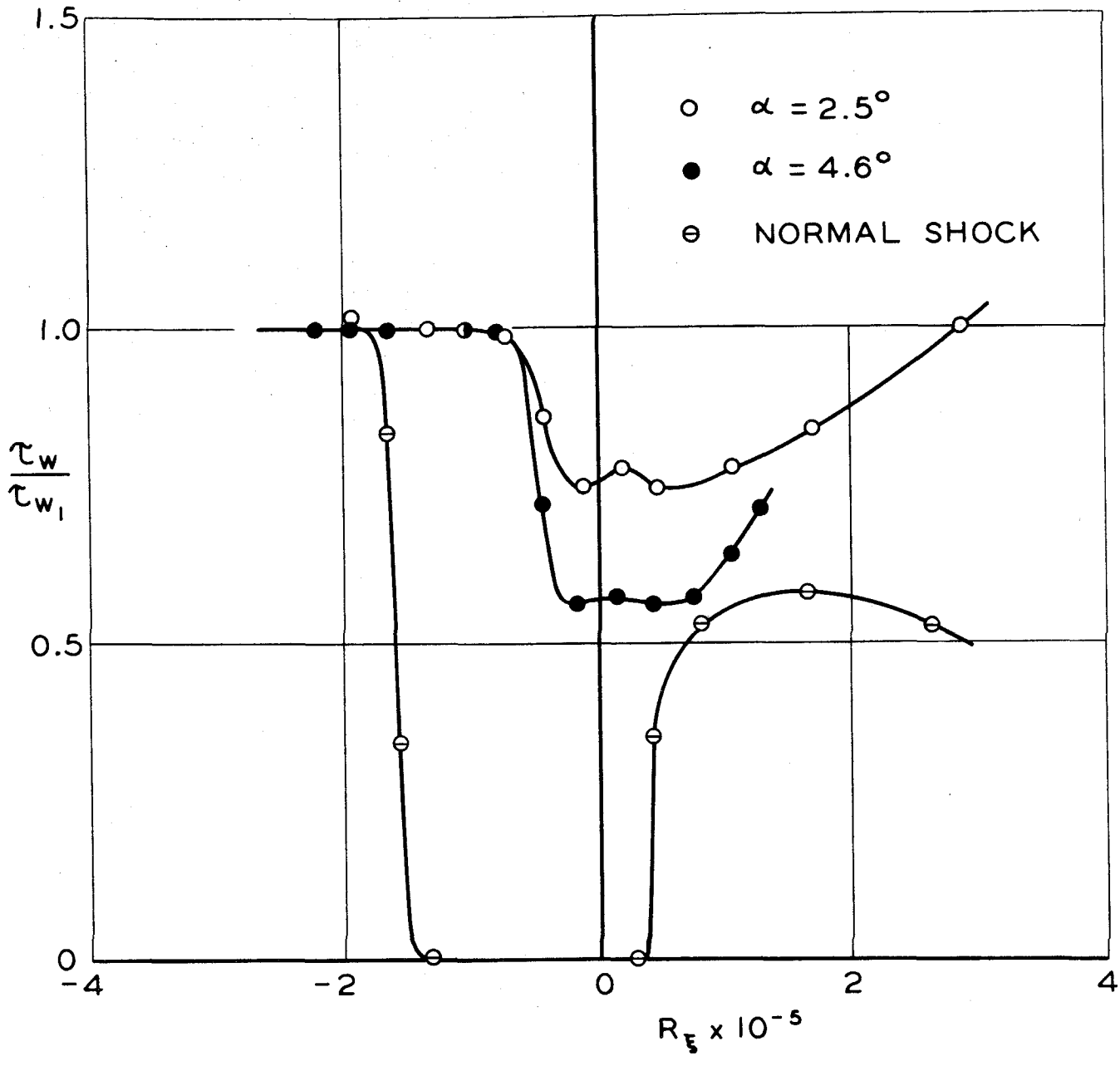

SHEAR STRESS ON SURFACE

$M_1 \doteq 1.48$ $R \doteq 1.2 \times 10^5$ CM.$^{-1}$

$\tau_{w_1} \doteq 1030$ DYN. CM.$^{-2}$

FIG. 29